Gas-Phase Reactivity of Cu^+ and Ag^+ with Glycerol: an Experimental and Theoretical Study

Laurence Boutreau,[†] Emmanuelle Léon,[†] Luis Rodríguez-Santiago,[†,§] Pierre Toulhoat,[‡] Otilia Mó,[||] and Jeanine Tortajada*[,†]

Laboratoire Analyse et Environnement, UMR 8587; Université d'Evry val d'Essonne, Bâtiment des Sciences, Boulevard F. Mitterrand, 91025 EVRY CEDEX, France, CEA SACLAY, DCC/DESD/SESD, Bâtiment 450, 91191 GIF/YVETTE CEDEX, France, and Departamento de Química, C-9, Universidad Autónoma de Madrid, Cantoblanco, 28049 Madrid, Spain

Received: January 14, 2002; In Final Form: July 11, 2002

The reactions between Cu^+ and Ag^+ metal cations and glycerol ($CH_2OH-CHOH-CH_2OH$) in the gas phase have been investigated by means of mass spectrometry and B3LYP density functional calculations. The $[glycerol,X]^+$ (X = Cu, Ag) complexes are formed in the ion source. The structures of several coordinations of the metal cation to glycerol have been determined at the B3LYP level. Calculations show that although the preferred attachment for Cu^+ involves a chelation between two hydroxyl oxygens of glycerol, a tricoordinated structure is obtained for Ag^+ complexation. The MIKE spectra of the $[glycerol,X]^+$ ions have also been analyzed and show that both complexes undergo fragmentation by different pathways. For $[glycerol,Ag]^+$, the most important fragmentation corresponds to the loss of glycerol process. However, this process is not observed for $[glycerol,Cu]^+$, where the major fragmentation corresponds to the elimination of water. The possible mechanisms leading to these fragmentations, and others observed only to a minor extent, have been studied using labeled glycer(ol-d_3) and calculations performed at the B3LYP level.

1. Introduction

The study of metal cation interactions with organic and bioorganic compounds in the gas-phase constitutes a very active domain of research. Presently, attempts to understand complicated biological processes that involve metal cations can be made by modeling substrate-metal ion interactions in the absence of solvent. Under such conditions, one may grasp the intrinsic properties of complexes formed in the gas phase, and in this area, mass spectrometry has become a available method of selection and a valuable tool in studying the gas-phase interactions of metal ions and various substrates.[1]

The cationization of neutral molecules by association with metal cations involves significant bond-activation effects, which can lead to specific bond cleavages observed in mass spectrometry experiments. On the other hand, with the current growing importance of computational chemistry in understanding the relationship between structure and activity, the accurate characterization of molecular structures using theoretical methods has proven to be a useful tool. Thus, studies of cationized compounds by combining molecular orbital calculations with experimental data lead to an improved description of intrinsic properties and activation mechanisms.

Lately, we have devoted particular attention to the reactions between Cu^+ and small compounds of biochemical relevance, such as formamide,[2] guanidine,[3] urea,[4] or phosphoric acid.[5] These studies were aimed at modeling the intrinsic complexation properties of several subunits of nucleic acids. Recently, increasing attention has been paid to studies concerning the cationization of carbohydrates.[6] In addition, saccharides, which are molecules that have a great number of stereoisomers, present many hydroxyl groups leading to the formation of several intramolecular hydrogen bonds. These features make it difficult to rationalize the fragmentation patterns observed in mass spectrometry experiments. Recently, we have devoted particular attention to the reaction between Cu^+ and glucose.[7] This apparently simple system presents a great number of modes of complexation, and so, a reasonable alternative is the study of smaller model systems, which present similar active sites. Thus, we have considered the study of the gas-phase reactions of glycerol ($HOCH_2CHOHCH_2OH$) with two metal monocations, namely Cu^+ and Ag^+ to be of interest. Glycerol, which is the most frequently used matrix for FAB experiments,[8] can compete for the metal cation with the substrate of interest, as shown by experimental results. Glycerol presents, as an additional interesting feature, three oxygen basic centers and several intramolecular hydrogen bonds, which can lead to several kinds of complexations and stabilizations. Thus, this system can model part of the interactions found in metal−saccharide ionized complexes.

Because Cu^+ plays an important role in biological media, considerable work has been devoted to the study of complexes between copper(I) and molecules of biological interest.[9] Cu^+ is widely distributed in the plant and animal worlds, and its redox chemistry is involved in a variety of oxidation processes. The silver(I) ion has long been used as a bactericide in the form of eye drops for newborns,[10] and some of its complexes show remarkable anti-microbial activity.[11] The silver(I) ion binds relatively strongly to α-amino acids, peptides, and proteins, but very little work[12] has been done on this subject. At a theoretical level, Cu^+ and Ag^+ present a d^{10} closed-shell ground state with an empty 4s orbital for Cu^+ and an empty 5s orbital for Ag^+.

* To whom correspondence should be addressed. E-mail: jeanine.tortajada@chimie.univ-evry.fr. Fax: (33) 1 69 47 76 55.

[†] Laboratoire Analyse et Environnement, UMR 8587; Université d'Evry val d'Essonne.

[‡] CEA SACLAY, DCC/DESD/SESD.

[§] Present adress: Departament de Química, Universitat Autònoma de Barcelona, Bellaterra 08193 Barcelona.

[||] Universidad Autónoma de Madrid.

10.1021/jp020092+ CCC: $22.00 © 2002 American Chemical Society
Published on Web 10/10/2002

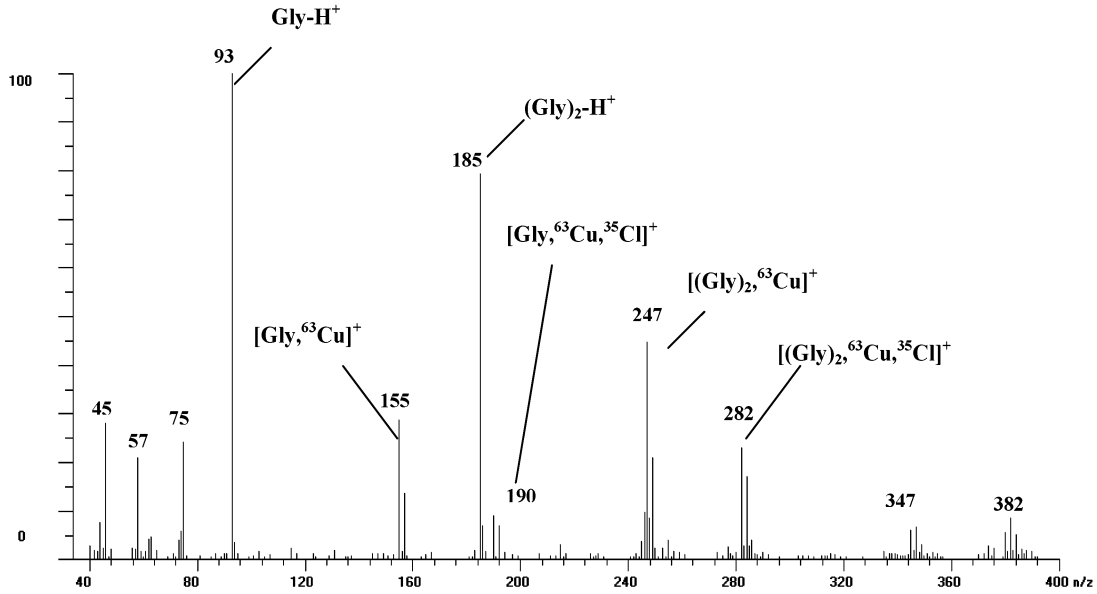

Figure 1. FAB spectrum of an aqueous solution of glycerol and $CuCl_2$.

Hence, it is reasonable to expect that the interaction of glycerol with these transition metal monocations should have important covalent contributions, as it has been found in reactions of Cu^+ with simple hydrocarbons or small nitrogen bases.[13] The promotion of both metal ions from the ground state ($3d^{10}$ for Cu^+ or $4d^{10}$ for Ag^+) to excited states (3d94s1 or 4d95s1, respectively) requires a considerable amount of energy;[14] thus, Cu^+ and Ag^+ react more by dissociative attachment rather than by bond insertion. Moreover, Cu^+ and Ag^+ form multicoordinated species[15] in the gas phase as generally found for transition metal cation compounds.

The aim of this paper is to present the most significant experimental findings of the gas-phase reactivity of $[glycerol,X]^+$ complexes (with X = Ag or Cu) based on mass-analyzed ionic kinetic energy spectroscopy (MIKES) experiments. The $[glycerol,X]^+$ ions are obtained in a fast atom bombardment (FAB) ion source. To complete the information on these systems, the MIKE spectra of the deuterated glycerol complexes were also studied. Finally, to offer a complete interpretation of the experimental findings, a reliable description of the potential energy surfaces of these systems has been performed using the B3LYP density functional method.

2. Experimental and Computational Methods

2.1 Experimental. The Fast Atom Bombardment (FAB) mass spectrometric measurements were recorded on a double-focusing ZAB−HSQ mass spectrometer (Fisons Instrument) of BEqQ configuration[16] (where B and E represent the magnetic and the electrostatic sectors, q a collision cell consisting on an r.f.-only quadrupole and Q a mass scanning quadrupole). This mass spectrometer is equipped with a FAB ion source using the following conditions: accelerating voltage 8 kV, neutral xenon beam 7 keV and neutral current of ~10 μA. Glycerol was dissolved in a few drops of a saturated aqueous metallic (silver or copper) salt solution. Few μL of the resulting mixture was transferred onto the FAB tip. The Ag^+ ions are formed from Ag^+ salt ($AgNO_3$), whereas the Cu^+ ions are likely formed from Cu^{2+} salt (e.g., $CuCl_2$, $2H_2O$) by oxidation/reduction processes, as has been previously postulated.[17] Silver and copper ions are seen in their natural abundance (51% ^{107}Ag/49% ^{109}Ag and 69% ^{63}Cu/31% ^{65}Cu).

The unimolecular reactions of the mass-selected organometallic ions, corresponding to $[glycerol, X]^+$ metastable ions (with X = Ag or Cu), which take place in the second field-free region (second FFR) behind the magnet, were studied by mass analyzed ion kinetics energy (MIKE) spectroscopy.[18] This technique consists of focusing the relevant organometallic ion magnetically into the second FFR and detecting the products of spontaneous fragmentations by scanning the electrostatic analyzer, E. The MIKE spectra were recorded at a resolving power of ~1000. For Collisionally Activated Decomposition (CAD) MS/MS spectra, the pressure of argon in the collision cell was adjusted so that the main beam signal was reduced by approximately 30%. Metallic salts, glycerol, and glycer(ol-d_3) are commercially available from Aldrich and were used without any further purification

2.2 Computational. Full geometry optimizations and harmonic vibrational frequency calculations of different species have been performed using the Becke's three-parameter nonlocal hybrid exchange potential with the nonlocal correlation functional of Lee, Yang, and Parr (B3LYP).[19] This approach is known to yield reliable geometries for a wide variety of systems, including many transition metal containing systems.[20−24]

Geometry optimizations have been carried out with the 6-311G(d,p) basis set for C, O and H. The Cu basis set is a ^{9s5p3d} contraction of the (14s9p5d) primitive set of Watchers [25] supplemented with one *f* function ($\alpha_f = 1.44$). The final basis set is of the form (14s9p5d1f)/[9s5p3d1f]. For Ag, we use the relativistic effective core potentials (RECP) developed by Hay and Wadt[26] (LANL2DZ). These RECP include the outermost core orbitals 4s and 4p in the valence shell. The valence basis set is a [3s3p2d] contraction of a (5s6p4d) primitive set of Hay and Wadt[26] supplemented with one set of f functions (α_f = 0.5897). This basis set will hereby be denoted as basis1. Harmonic vibrational frequencies of the different stationary points of the potential energy surface (PES) have been calculated at the same level of theory in order to identify the local minima as well as to estimate the corresponding zero point energies (ZPE).

Final energies have been obtained at the B3LYP level using the following basis set. For C, O, and H we use the 6-311G-(2df,2p) basis set. The Cu basis set is the same (14s9p5d)/^{9s5p3d} basis set of Wachters supplemented with two sets of f (α_f = 2.88, 0.72) and one set of g ($\alpha_g = 1.44$) polarization functions. For Ag, we have used the (5s6p4d)/[3s3p4d] basis set (by

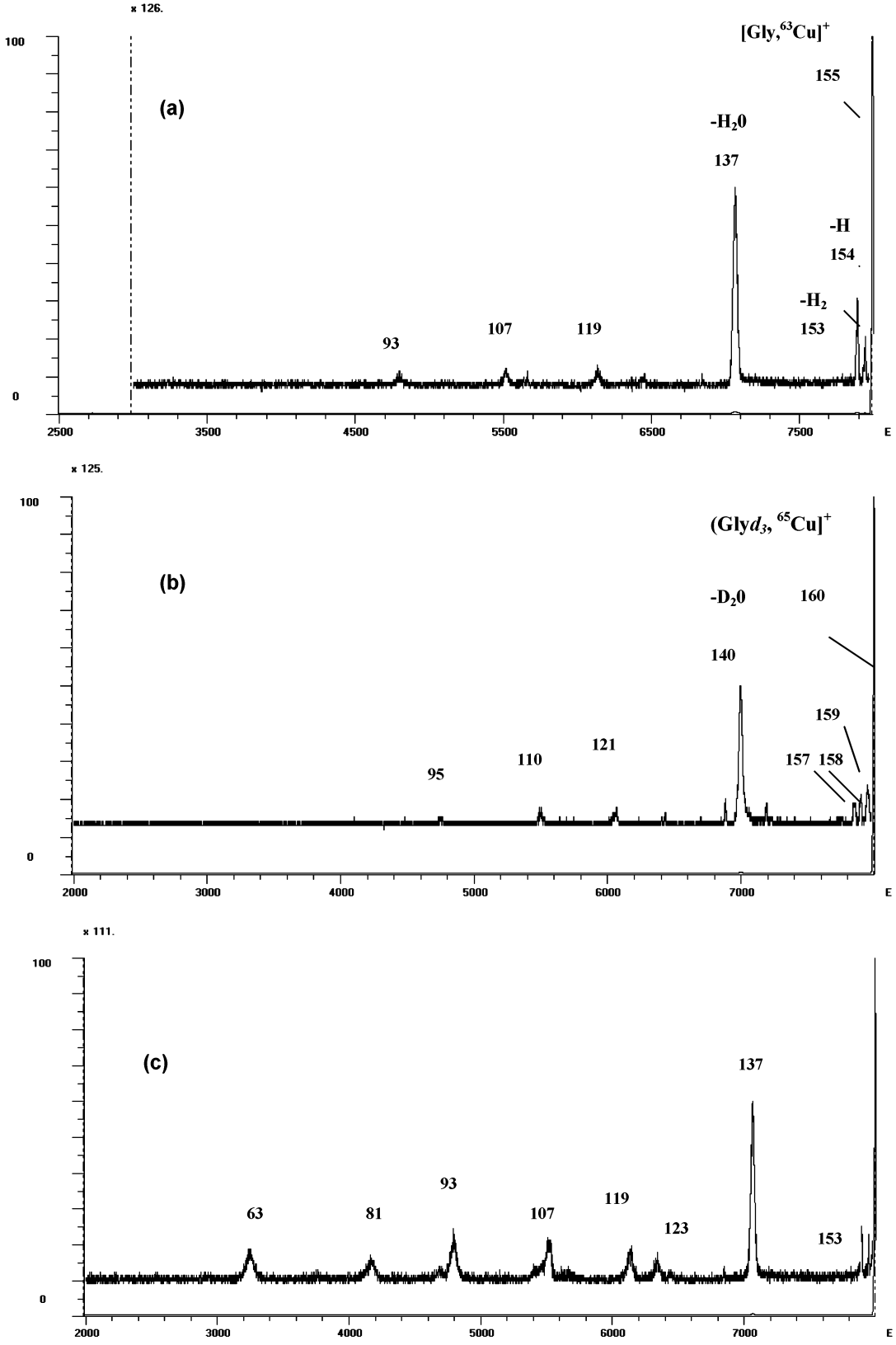

Figure 2. (a) MIKE spectrum of the [glycerol,^{63}Cu]$^+$ complex at *m*/*z* 155. (b) MIKE spectrum of the [glycer(ol-*d3*),^{65}Cu]$^+$ complex at *m*/*z* 160. (c) MIKE-CAD spectrum of the [glycerol,^{63}Cu]$^+$ complex at *m*/*z* 155.

decontracting the d functions) supplemented with two sets of f (α_f = 1.545, 0.386) and one set of g (α_g=0.504) polarization functions. Hereafter, this basis set will be referred as basis 2.

The basis set superposition error (BSSE) has not been considered in the present study because for DFT methods, this error is usually small using a flexible basis set expansion, as has been previously reported.[27]

To study the nature of the Cu−O and Ag−O bonds and, in general, the bonding features of the complexes under investigation, we have used the atoms in molecules (AIM) theory of

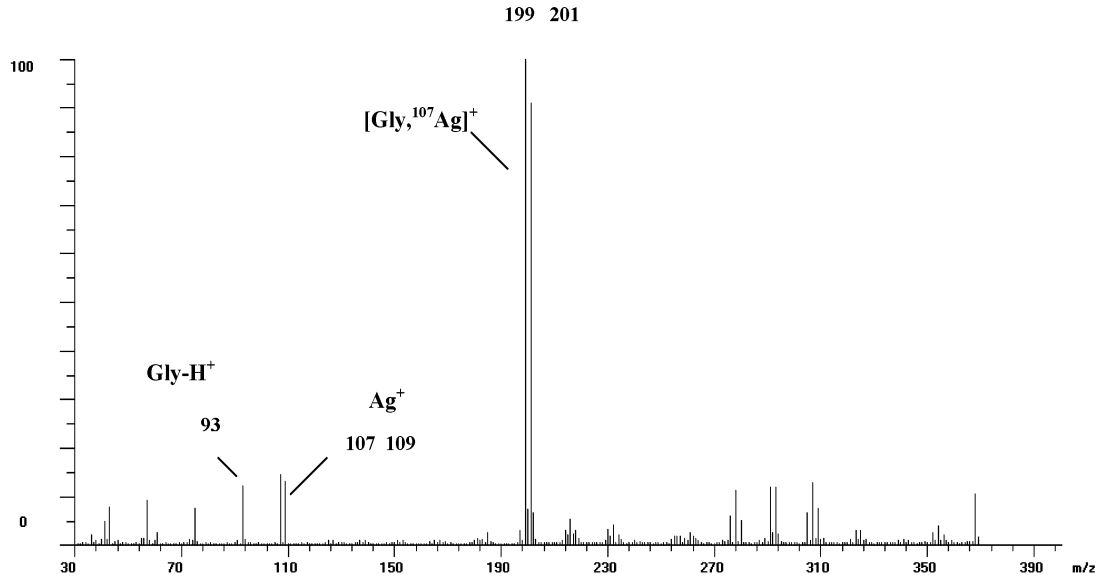

Figure 3. FAB spectrum of an aqueous solution of glycerol and $AgNO_3$.

Bader.[28] We have located the bond critical points (i.e., points where the electron density function, $\rho(r)$ is minimum along the bond path and maximum in the other two directions). The Laplacian of the density, $\nabla^2\rho(r)$, as has been shown in the literature, identifies regions of the space wherein the electronic charge is locally depleted ($\nabla^2\rho > 0$) or built up ($\nabla^2\rho < 0$). The former situation is typically associated with interactions between closed-shell systems (ionic bonds, hydrogen bonds, and van der Waals interactions), whereas the latter characterizes covalent bonds, where the electron density concentrates in the internuclear region.

Calculations were carried out using the GAUSSIAN-98 series of programs.[29] The AIM analysis was performed using AIMPAC[30] series of programs.

3. Results and Discussion

3.1 Experimental Study. *FAB-MS Spectrum of Glycerol with the Aqueous Solution of $CuCl_2$.* Figure 1 shows the FAB mass spectrum that results from the fast atom bombardment of the mixture containing glycerol and $CuCl_2$. Due to the acidity of the aqueous solution of $CuCl_2$, the FAB spectrum presents predominant protonated species that correspond to [glycerol,H^+] (at *m*/*z* 93), [(glycerol)$_2$,H^+] (at *m*/*z* 185) and also fragment ions at *m*/*z* values under 93. These ions have been studied previously,[11a] and therefore, they will not be discussed here. Both peaks corresponding to copper adduct ions, [glycerol,-Cu]$^+$ at *m*/*z* 155 and [(glycerol)$_2$,Cu]$^+$ at *m*/*z* 247, are very intense. Copper ions are seen in their natural abundance, i.e., 69% ^{63}Cu and 31% ^{65}Cu. The existence of these two isotopes leads to an easy identification of copper-containing ions. In addition, the spectrum shows two other ions at *m*/*z* 190 and 282 that correspond to the interaction of $CuCl^+$ with one and two molecules of glycerol, respectively. Although we use a Cu^{2+} salt, no dicharged copper complexes are observed and Cu^+ ions are formed by oxidation/reduction either in solution or in gas phase in the gaseous plasma formed under FAB desorption.

Unimolecular Reactivity of the [Glycerol,Cu]$^+$ Adduct Ion. The MIKE spectrum of the [glycerol,Cu]$^+$ complex presented in Figure 2a shows that the *m*/*z* 155 ion undergoes several fragmentations. The major fragmentation corresponds to the elimination of H_2O at *m*/*z* 137. The [glycerol,Cu]$^+$ ion shows two other important losses, namely those of H$\cdot$ at *m*/*z* 154 and H_2 at *m*/*z* 153. Other smaller peaks are also obtained and correspond to the elimination of two water molecules at *m*/*z* 119, CH_2O and H_2O at *m*/*z* 107 and a peak at *m*/*z* 93 that corresponds to $[CuCH_2O]^+$. The collision-activation dissociation (MIKE/CAD spectrum displayed in Figure 2c) shows in addition the formation of Cu^+ (*m*/*z* 63) and $[H_2O-Cu]^+$ (*m*/*z* 81).

To have some information on the mechanisms for the unimolecular reactions we have examined the behavior of the [glycer(ol-d_3)^{65}Cu]$^+$ (*m*/*z* 160)complex. We present the spectrum corresponding to the [glycerol,^{65}Cu]$^+$ complex to discard the possible interferences coming from [(glycerol-H_2),^{63}Cu]$^+$. The base peak of the obtained mass spectrum (see Figure 2b) at *m*/*z* 140 corresponds to the elimination of D_2O, and no loss of HDO or H_2O is observed thus, indicating that the hydrogen atoms involved in this fragmentation are hydroxyl hydrogen atoms. Moreover, the loss of three units at *m*/*z* 157 demonstrates that the hydrogen atoms implicated in the H_2 loss arise from OH and CH (or CH_2) groups. Apart from these fragmentations, peaks corresponding to the loss of H$\cdot$ and D$\cdot$ are also observed at *m*/*z* 159 and *m*/*z* 158, respectively.

FAB-MS Spectrum of Glycerol Dissolved in an Aqueous Solution of $AgNO_3$. As shown in Figure 3, the FAB mass spectrum of glycerol, dissolved in an aqueous solution containing $AgNO_3$ produces abundant [glycerol, Ag]$^+$ adduct ion at *m*/*z* 199/201, which is the base peak of the FAB-MS spectrum. Silver ions are seen in their natural abundance, i.e., 51% ^{107}Ag and 49% ^{109}Ag. In our experimental conditions, several other silver/organic complexes were also observed. They correspond to the formation of organometallic cations, which contain one, two, or three silver atoms interacting with glycerol and glycerol fragments. For instance, the ions at *m*/*z* 291/293 and at *m*/*z* 305/307/309 correspond respectively to [(glycerol)$_2$,Ag]$^+$ and [(glycerol-H),2Ag]$^+$ complexes. In addition, all of the peaks observed at *m*/*z* values under 107 correspond to the protonation of glycerol (*m*/*z* 93) and their fragment ions.

Unimolecular Reactivity of the [Glycerol,Ag]$^+$ Adduct Ion. The unimolecular behavior of [glycerol,Ag]$^+$ ions formed by FAB was investigated from the MIKE spectrum shown in Figure 4a. We present the spectrum corresponding to the [glycerol,^{109}Ag]$^+$ complex to discard the possible interferences coming from [(glycerol-H_2),^{107}Ag]$^+$. It can be observed in this spectrum that the *m*/*z* 201 ion undergoes fragmentation by four pathways. The major reaction corresponds to the loss of the

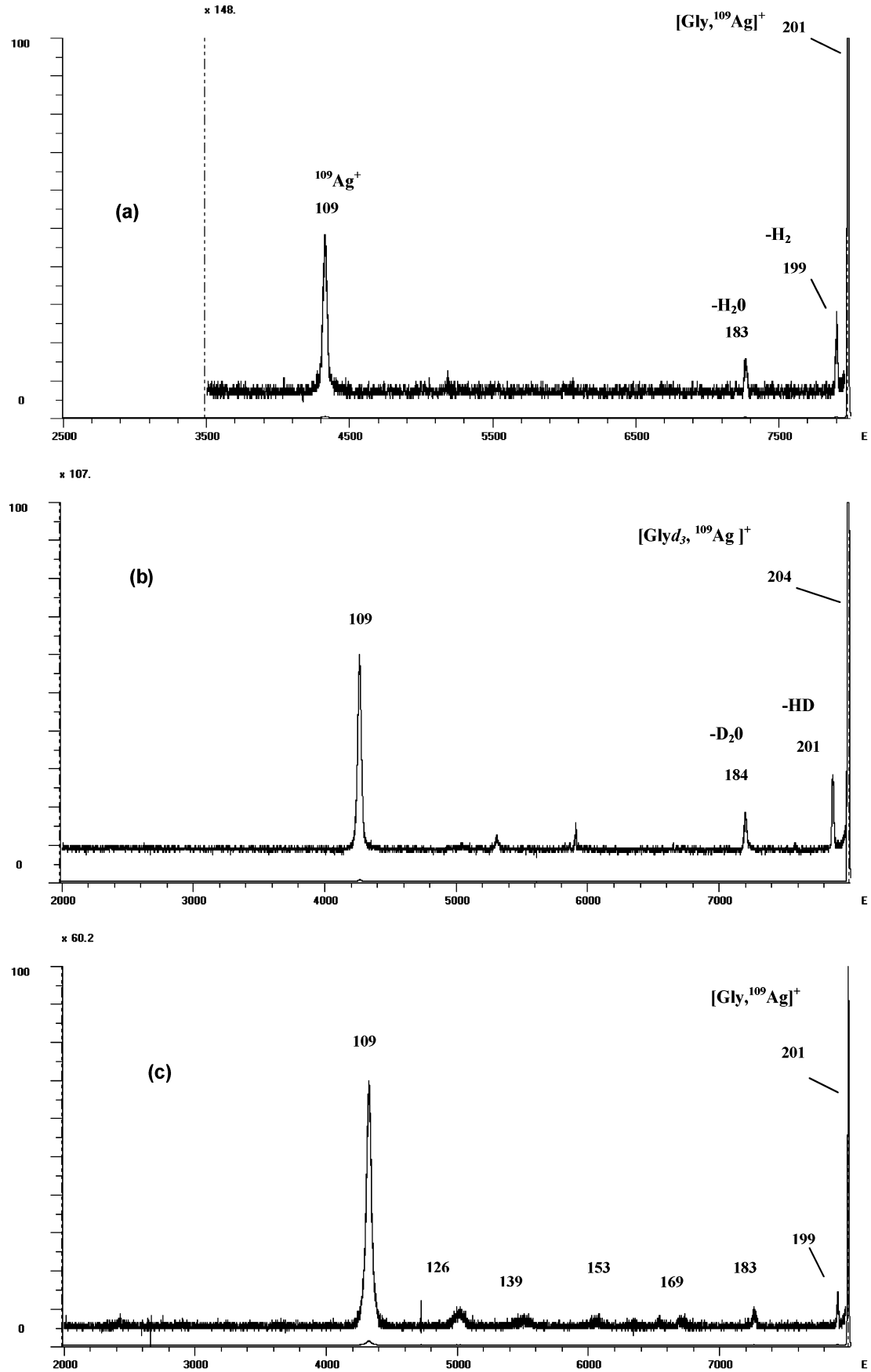

Figure 4. (a) MIKE spectrum of the [glycerol,^{109}Ag]$^+$ complex at *m*/*z* 201. (b) MIKE spectrum of the [glycer(ol- d_3),^{109}Ag]$^+$ complex at *m*/*z* 201. (c) MIKE-CAD spectrum of the [glycerol,^{109}Ag]$^+$ complex at *m*/*z* 201.

ligand as shown by the presence of Ag^+ cation at *m*/*z* 109 (base peak of the MIKE spectrum). This reaction process was not observed in the case of the [glycerol,Cu]$^+$ adduct. Besides this fragmentation, the elimination of H_2 leading to the ion at *m*/*z*

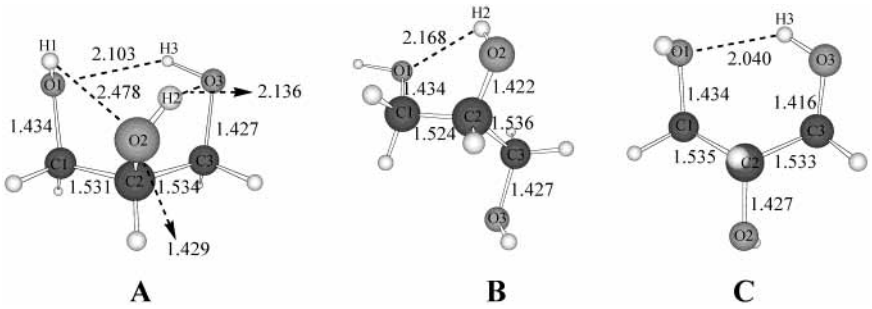

Figure 5. Optimized geometries for neutral of glycerol at the B3LYP/basis1 level. Distances are in Angströms and angles in degrees.

TABLE 1: Total Energies, ZPE (in Hartree), Relative Energies (in kJ mol^{-1}) of the Stationary Points of Neutral Glycerol and Entropy (in cal/K mol)

system	absolute *E* B3LYP/basis1	ZPE	$S°_{298}$	*E*rel[a] B3LYP/basis1	absolute *E* B3LYP/basis2	*E*rel[a] B3LYP/basis2
Glycerol *A*	−344.891917	0.119943	79.4	0 (0)	−344.911715	0 (0)
Glycerol *B*	−344.885593	0.118761	82.4	17 (13)	−344.905370	17 (13)
Glycerol *C*	−344.885264	0.119123	81.2	17 (15)	−344.904673	18 (16)

[a] The *E*rel+ZPE energies are shown in parentheses. In both cases, the ZPE and $S°_{298}$ have been determined at the B3LYP/basis1 level.

TABLE 2: Charge Densities ρ (in e au^{-3}) and Laplacian $\nabla 2(\rho)$ (in e au^{-5}) of the Charge Densities Evaluated at the Corresponding Bond Critical Points (bcp's) of Some Bonds of the Different Isomers of Glycerol and [Glycerol,X]$^+$

	C1−C2		C2−C3		C1−O1		C2−O2		C3−O3		O1-X		O2-X		O3-X		O1−H3		O3−H2	
	ρ	$\nabla 2\rho$	ρ	$\nabla 2\rho$	ρ	$\nabla 2\rho$	ρ	$\nabla 2\rho$	ρ	$\nabla 2\rho$	ρ	$\nabla 2\rho$	ρ	$\nabla 2\rho$	ρ	$\nabla 2\rho$	ρ	$\nabla 2\rho$	ρ	$\nabla 2\rho$
A	0.252	−0.597	0.250	−0.583	0.248	−0.460	0.253	−0.508	0.253	−0.496							0.021	0.070	0.021	0.085
B	0.255	−0.615	0.250	−0.583	0.246	−0.436	0.258	−0.522	0.251	−0.455										
C	0.250	−0.588	0.251	−0.588	0.246	−0.447	0.252	−0.475	0.261	−0.533							0.024	0.080		
1Cu+	0.242	−0.549	0.242	−0.547	0.225	−0.366	0.259	−0.521	0.223	−0.340	0.092	0.554			0.093	0.576				
2Cu+	0.240	−0.540	0.240	−0.540	0.220	−0.327	0.263	−0.560	0.219	−0.321	0.095	0.590			0.095	0.593				
3Cu+	0.256	−0.623	0.255	−0.623	0.231	−0.371	0.233	−0.381	0.254	−0.483	0.064	0.310	0.079	0.441					0.024	0.100
4Cu+	0.255	−0.616	0.253	−0.616	0.228	−0.337	0.227	−0.343	0.262	−0.527	0.073	0.385	0.071	0.367						
5Cu+	0.251	−0.593	0.249	−0.583	0.258	−0.504	0.217	−0.241	0.283	−0.604			0.089	0.525			0.026	0.091		
6Cu+	0.250	−0.597	0.247	−0.573	0.239	−0.391	0.264	−0.518	0.228	−0.412					0.109	0.698	0.048	0.163		
1Ag+	0.254	−0.608	0.258	−0.640	0.243	−0.445	0.241	−0.434	0.241	−0.427	0.040	0.178	0.041	0.194	0.030	0.086	0.030	0.086		
2Ag+	0.254	−0.613	0.254	−0.614	0.231	−0.342	0.265	−0.583	0.230	−0.342	0.051	0.266			0.051	0.266				
3Ag+	0.257	−0.630	0.254	−0.615	0.234	−0.363	0.236	0.383	0.254	−0.478	0.043	0.214	0.050	0.265					0.024	0.101
4Ag+	0.260	−0.643	0.252	−0.606	0.234	−0.361	0.231	−0.348	0.265	−0.566	0.048	0.233	0.047	0.237						
5Ag+	0.254	−0.609	0.252	−0.604	0.259	−0.527	0.229	−0.299	0.289	−0.618			0.052	0.266			0.030	0.086		
6Ag+	0.252	−0.604	0.248	−0.580	0.239	−0.382	0.263	−0.526	0.223	−0.305					−0.065	0.351	0.045	0.149		

199 is also observed, as in the case of the [glycerol,Cu]$^+$ ion, and a weak peak at *m*/*z* 183 corresponding to the loss of H_2O. Another difference with the MIKE spectrum of [glycerol,Cu]$^+$ is that in the case of Ag^+ the elimination of H$\cdot$ is not observed.

We have also studied the behavior of the corresponding [glycer(ol-d_3) ^{109}Ag]$^+$ complex. The results are very similar to that found for the case of the [glycerol,Cu]$^+$ complex, that is, the [glycer(ol-d_3) ^{109}Ag]$^+$ ion losses three units (HD) to give a peak at *m*/*z* 201 and D_2O at *m*/*z* 184 (see Figure 4b). Under collision activation, we can observe in Figure 4c, the presence of others minor ions, Ag^+ remaining the major ion.

To rationalize the experimental findings, including the differences found in the reactivity of copper and silver complexes, we have studied the most important features of [glycerol,X]$^+$ potential energy surfaces by means of the B3LYP method. We have considered the possible coordination modes of Cu^+ and Ag^+ to glycerol then, we have explored the possible mechanisms leading to the most important experimentally observed fragments.

3.2 Theoretical Study. *Neutral Glycerol Species.* Due to the large number of possible rotations, glycerol ($CH_2OH-CHOH-CH_2OH$) presents many possible conformations. The conformational study of glycerol is not the objective of this paper, and an exhaustive analysis of glycerol conformations has been already accomplished by other authors.[31,32]

We have selected three conformations for neutral glycerol. Optimized B3LYP geometries and energies of these three structures are given in Figure 5 and Table 1, respectively.

Structure **A** is the most stable structure of glycerol. The three oxygen atoms of this isomer are in position syn, which favors the formation of three hydrogen bonds (2.103, 2.136, and 2.478 Å) between the three-hydroxyl groups. The strength and stability of the intramolecular hydrogen bonds (IHB) can be analyzed using the charge density at the corresponding bond-critical points (bcps). Table 2 shows the charge density and laplacian of the charge densities at the bond critical points of selected bonds of the different isomers of glycerol and [glycerol,X]$^+$. In structure **A**, several IHBs have been characterized. It can be observed that the stability of this structure is principally due to two strong IHBs (H2...O3 and H3...O1) as reflected by the charge density ρ (0.021 e au^{-3}). Structures **B** and **C** are almost degenerated and lie 17 and 18 kJ mol^{-1}, respectively, above the structure **A** at the B3LYP/basis2 level. Only one hydrogen bond is possible in these structures (2.168 Å for **B** and 2.040 Å for **C**). Because different metal complexations can be considered: on the triple-, double-, or single-basic center, we have considered these three structures for the theoretical study on complexation of glycerol by Cu^+ and Ag^+.

Cationization of Glycerol with Cu$^+$. Structures, Bonding, and Affinity. Several structures corresponding to the interaction of

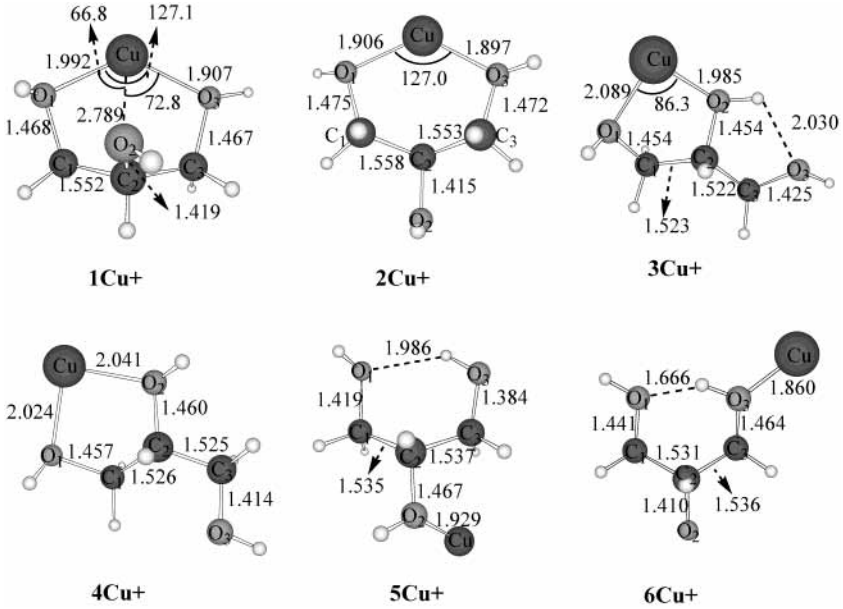

Figure 6. Optimized geometries for the different minima of the [glycerol,$Cu]^+$ complex at the B3LYP/basis1 level. Distances are in Angströms and angles in degrees.

TABLE 3: Total Energies, ZPE (in Hartree), Relative Energies (in kJ mol^{-1}) of the Stationary Points of Copper Complexes and Entropy (in cal/K mol)

system	absolute *E* B3LYP/basis1	ZPE	$S°_{298}$	*E*rel[a] B3LYP/basis1	absolute *E* B3LYP/basis2	*E*rel[a] B3LYP/basis2
$1Cu^+$	−1985.116906	0.121275	89.2	0 (0)	−1985.141852	0 (0)
$2Cu^+$	−1985.108594	0.121075	89.9	22 (21)	−1985.133803	21 (21)
$3Cu^+$	−1985.104545	0.120522	92.7	32 (30)	−1985.126784	39 (37)
$4Cu^+$	−1985.098338	0.120255	93.6	49 (46)	−1985.121143	54 (52)
$5Cu^+$	−1985.072977	0.119628	94.2	115 (111)	−1985.097326	117 (113)
$6Cu^+$	−1985.087179	0.120650	93.8	78 (76)	−1985.108231	88 (86)

[a] The *E*rel+ZPE energies are shown in parentheses. In both cases, the ZPE and $S°_{298}$ have been determined at the B3LYP/basis1 level. The entropy of Cu^+, $S°_{298}$ = 38.3 cal/K mol.

Cu^+ with the different basic sites of glycerol have been considered. The interaction of Cu^+ with a neutral molecule results principally from electrostatic and charge-transfer contributions. The most favorable binding sites are therefore the electron-rich oxygen atoms. Thus, the first criterion that we have retained is the maximization of such interactions through multidendate bindings, and the second criterion is to preserve intramolecular hydrogen bonds as much as possible.

Figure 6 shows the optimized structures for the [glycerol,$Cu]^+$ adduct. Among all of the possibilities considered, these structures have been characterized as minima. They correspond, as mentioned above, to different modes of cationization involving: (a) the three basic sites of the neutral glycerol (only available for conformation **A**), (b) two oxygen atoms of neutral glycerol and (c) only one oxygen atom of neutral glycerol. The computed total energies as well as the relative stabilities of these species obtained at the B3LYP level are summarized in Table 3.

The most stable [glycerol,$Cu]^+$ complex, $\mathbf{1Cu}^+$, corresponds to a chelated structure in which the metal cation interacts with two oxygen atoms leading to a complex having three different Cu−O distances: two short bonds O1−Cu and O3−Cu (1.922 and 1.907 Å respectively) and a longer distance between O2 and Cu (2.789 Å) that seems to preclude a bonding interaction. Moreover, it can be observed in Figure 6 that the values of the OCuO angles also suggest a dicoordinated structure because we have two similar bonds (66.8° and 72.8°) and one longer angle (127.1°). When Cu^+ ion binds to the most stable structure of glycerol, hydrogen atoms rotate to avoid repulsive interactions between positively charged hydrogen atoms and the copper ion, and consequently, the IHBs disappear. The two Cu−O bonds have an important covalent character, as illustrated by the charge density at the bcp's (0.092 e au^{-3}). One can assume that the dominant contribution of the O-hybrid orbital and the appropriate sd hybrid orbital of Cu^+ permit a dative bond, which involves the lone pair of the two basic centers O1 and O3. The interaction with the third oxygen atom O2 is very weak, as corroborated by the absence of a bond critical point. After complexation, an activation of neighboring bonds is observed. Two C−O bonds lengthen (0.034 Å for the C1−O1 bond and 0.040 Å for the C3−O3 bonds) with regard to their values in neutral glycerol **A**. However, the C2−O2 bond is slightly shortened (0.010 Å). In addition, we observed an elongation of both the C1−C2 and C2−C3 bonds of about 0.02 Å. In summary, it appears that in this $\mathbf{1Cu}^+$ species, Cu^+ is strongly dicoordinated with O1 and O3 oxygen atoms, and the interaction with the third oxygen (O2) is weak and essentially electrostatic in nature. These bonding characteristics are mirrored in the topological analysis (see Table 2).

The rotation of the central hydroxyl group of $\mathbf{1Cu}^+$ leads to a less stable structure, namely $\mathbf{2Cu}^+$. The cost for the interaction loss with O2 is about 21 kJ mol^{-1}. It can be observed that the resulting $\mathbf{2Cu}^+$ structure has almost C_s symmetry, in that both Cu−O distances very similar (ca. 1.906 and 1.897 Å). Once more, the cationization induces an elongation of the C−O bonds directly involved in the metal interaction (about 0.04 Å) as well as the C−C bonds (ca. 0.02 Å), whereas the C2−O2 bond length is shortened.

TABLE 4: Binding Energies (D_0 and D_e) of Copper Complexes (in kJ mol^{-1})

system	D_0 B3LYP/basis1	D_0 B3LYP/basis2	D_e B3LYP/basis2
$1Cu^+$	323	336	333
$2Cu^+$	301	315	312
$3Cu^+$	290	297	295
$4Cu^+$	274	282	281
$5Cu^+$	207	219	220
$6Cu^+$	245	248	246

The **3Cu**$^+$ structure lies 39 kJ mol^{-1} above **1Cu**$^+$ and corresponds to the metal cation interacting with two oxygen atoms of adjacent hydroxyl groups, namely O1 and O2. It is worth noting that in comparison with the **2Cu**$^+$ structure, weaker O−Cu$^+$ bonds are present (2.098 and 1.985 Å, respectively, instead of 1.906 and 1.897 Å). The hydrogen bond, H2−O3, is present in the **3Cu**$^+$ isomer and in comparison with neutral species, this hydrogen bond is slightly reinforced (going from 0.021 to 0.024 e au^{-3} for ρ and 0.085 to 0.100 e au^{-5} for $\nabla^2\rho$). Thus, the attachment of the copper ion to O2 polarizes the electron charge density of the oxygen atom toward the metal ion. As a consequence, O2 presents a more acidic character becoming a better hydrogen donor. From **3Cu**$^+$, the rotation of the C2−C3 bond leads to the **4Cu**$^+$ isomer**,** which is also a five-member ring structure. The cost for the hydrogen bond loss is about 15 kJ mol^{-1}.

Finally, monocoordination was also considered. The **5Cu**$^+$ structure corresponds to the complexation of neutral species **C**, where Cu$^+$ is exclusively associated with the central oxygen atom O2 (with a bond length of 1.929 Å). This complex lies 117 kJ mol^{-1} above **1Cu**$^+$. It can be observed that the C2−O2 bond length increases by about 0.04 Å, as expected, regarding the corresponding structure of neutral glycerol. As in the case of **3Cu**$^+$, complexation induces a slight reinforcement of the hydrogen bond H3−O1. This is reflected once more in the distance and therefore in the charge density at the bcp.

The **6Cu**$^+$ structure lies 88 kJ mol^{-1} above the most stable one. This structure corresponds to the Cu$^+$ ion interacting with the O3 oxygen atom. As in the **3Cu**$^+$ isomer, the electron density of O3 is polarized toward the metal cation and therefore the oxygen atom becomes more acid. In this case, this behavior is even more important, the hydrogen bond distance (H3−O1) being only 1.666 Å.

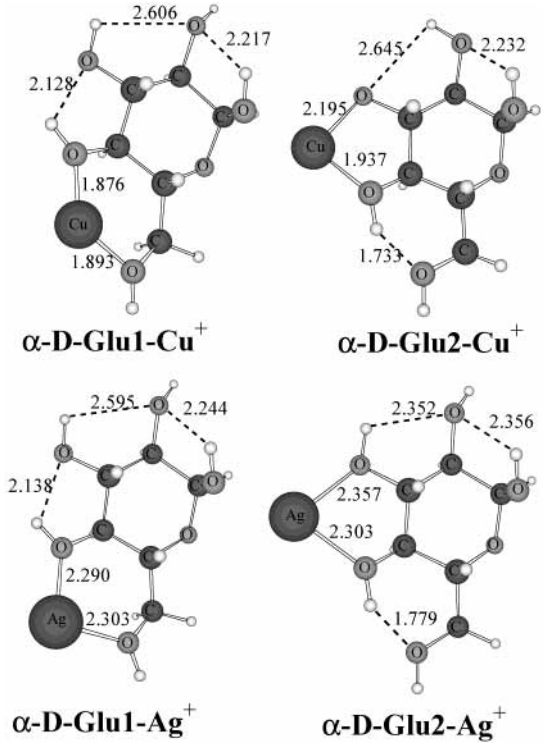

Figure 8. Optimized structures for copper and silver complexes of α-D-Glucose at the B3LYP/6-31G* and B3LYP/LANL2DZ. Distances are in Angströms.

Taking the most stable conformation of glycerol, **A**, as a reference, the binding energies for the six organometallic adducts have been calculated and are reported in Table 4. It is important to note that D_0 corresponds to the uncorrected binding energy, whereas D_e is the binding energy including the Zero Point Energy (ZPE) corrections obtained from B3LYP/basis1 vibra-

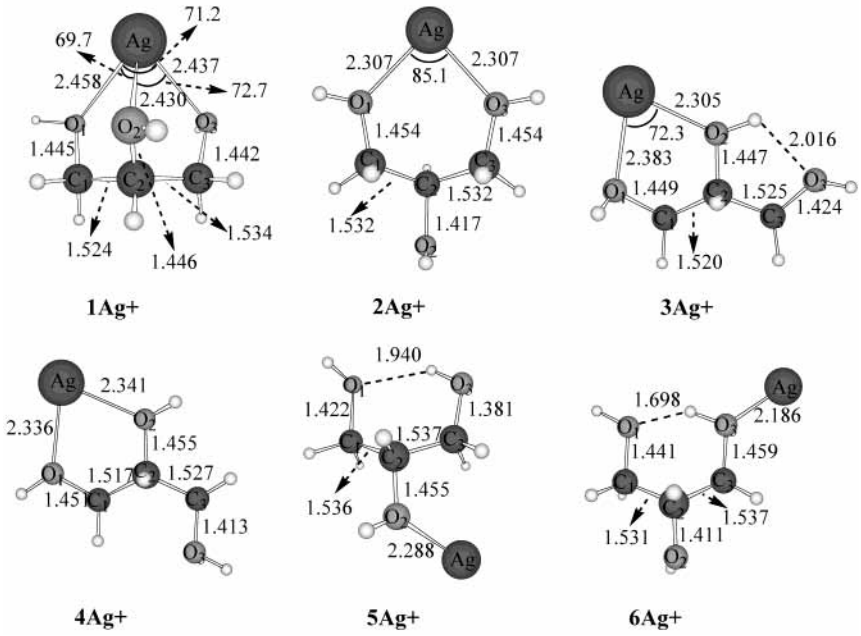

Figure 7. Optimized geometries for the different minima of the [glycerol,Ag]$^+$ complex at the B3LYP/basis1 level. Distances are in Angströms and angles in degrees.

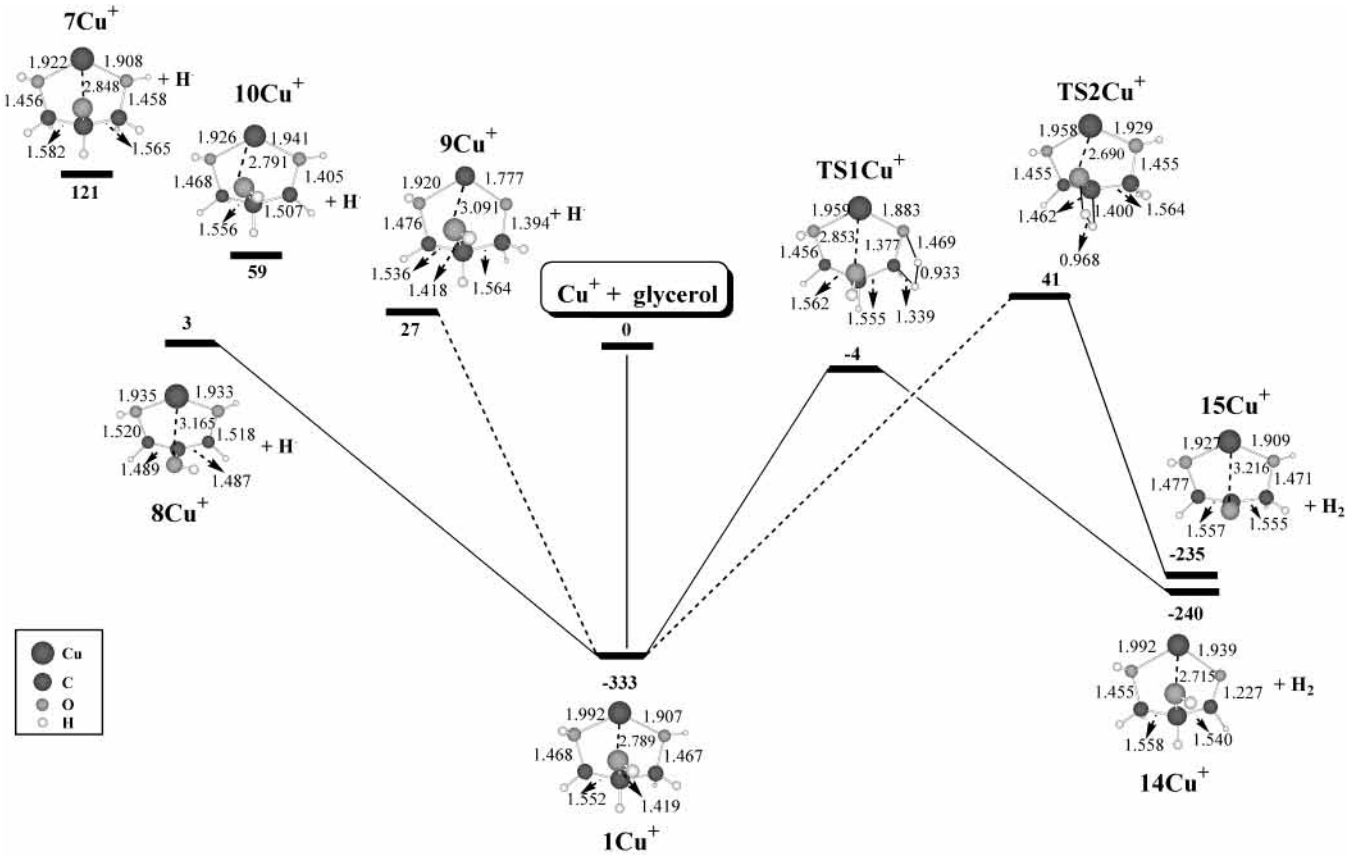

Figure 9. Schematic representation of the potential energy surface associated with several unimolecular reactions of [glycerol,$Cu]^+$ leading to the loss of H· and H_2. Distances are in Angströms and relative energies are in kJ mol^{-1}. B3LYP/basis2 + ZPE energies are shown.

TABLE 5: Total Energies, ZPE (in Hartree), Relative Energies (in kJ mol^{-1}) of the Stationary Points of Silver Complexes and Entropy (in cal/K mol)

system	absolute *E* B3LYP/basis1	ZPE	$S°_{298}$	*E*rel[a] B3LYP/basis1	absolute *E* B3LYP/basis2	*E*rel[a] B3LYP/basis2
$1Ag^+$	−490.452958	0.120335	93.5	0 (0)	−490.471532	0 (0)
$2Ag^+$	−490.437516	0.119563	100.3	40 (38)	−490.456250	40 (38)
$3Ag^+$	−490.446912	0.120060	97.6	16 (15)	−490.465522	16 (15)
$4Ag^+$	−490.441589	0.119754	96.4	30 (28)	−490.460201	30 (28)
$5Ag^+$	−490.414953	0.118696	97.6	100 (95)	−490.434740	97 (92)
$6Ag^+$	−490.428081	0.120058	97.5	65 (65)	−490.446929	65 (64)

[a] The *E*rel+ZPE energies are shown in parentheses. In both cases, the ZPE and $S°_{298}$ have been determined at the B3LYP/basis1 level. The entropy of Ag^+, $S°_{298}$ = 39.9 cal/K mol.

tional frequency calculations. It can be observed that the binding energy is correlated with the degree of coordination of the metal ion. For the **1Cu**$^+$ adduct De is 333 kJ mol^{-1}, similar to the values obtained for other Cu^+-organic complexes such as Cu^+-glycine[33] (303 kJ mol^{-1} at the B3LYP/6-311+G(2f,2d,2p)//B3LYP/6-31G* level) or Cu^+-guanidine[3] (326 kJ mol^{-1} calculated at the same level that Cu^+-glycerol). The binding energy for dicoordinated complexes **2Cu**$^+$, **3Cu**$^+$, and **4Cu**$^+$ are 312, 295, and 281 kJ mol^{-1}, respectively. For comparison, $\Delta G°_{298}$ for the formation of $Cu(MeOH)_2^+$ has been evaluated by Deng and Kebarle to be about 279 kJ mol^{-1}.[34] The binding energy for the monoliganded species **6Cu**$^+$ and **5Cu**$^+$ falls to 243 and 220 kJ mol^{-1}, respectively. Due to the reinforcement of the hydrogen bonding induced by the metal in the **5Cu**$^+$ structure, this last value is somewhat larger than that found for methanol-Cu^+ (176 kJ mol^{-1}).[35] It is worth noting that D_e increases when increasing the basis set, going from 321 kJ mol^{-1} at the B3LYP/basis1 level to 335 kJ mol^{-1} at the B3LYP/basis2 one for the **1Cu**$^+$ structure. The same trends are observed in all of the studied copper complexes, showing that improving the description of the Cu^+-glycerol system leads to a larger stabilization than the decreasing of the basis set superposition error when increasing the basis set. The entropy effects for the complexation reaction ($\Delta S°$) were evaluated from the vibrational frequencies calculations. The resulting entropy values are given in Tables 1 and 3. From these values, the entropy changes for the formation of copper complexes (ranging from −25.3 to −29.6 cal/K mol).

Cationization of Glycerol with Ag^+. Structures, Bonding, and Affinity. In the case of silver complexes, we have considered the same structures as in the case of copper complexes. The six optimized isomers of [glycerol, $Ag]^+$ are shown in Figure 9. Total energies of these species as well as their relative stabilities are summarized in Table 5. The most stable [glycerol, $Ag]^+$ complex corresponds to a tricoordinated structure, **1Ag**$^+$, in which the metal cation is interacting with the three oxygen atoms with similar bond distances (2.430, 2.437, and 2.458 Å). Furthermore, the three OAgO angles are also very similar, 69.7°, 71,2°, and 72.7° in agreement with a tricoordinated structure. Cationization induces the lengthening of the three C−O bonds

TABLE 6: Binding Energies (D_0 and D_e) of Silver Complexes (ion kJ mol^{-1})

system	D_0 B3LYP/basis1	D_0 B3LYP/basis2	D_e B3LYP/basis2
$1Ag^+$	229	225	224
$2Ag^+$	188	185	186
$3Ag^+$	213	209	209
$4Ag^+$	199	195	196
$5Ag^+$	129	129	132
$6Ag^+$	163	161	160

(0.011 Å for C1−01, 0.017 Å for C2−O2, and 0.015 Å for C3−O3). We can observe that the electronic density (ρ) at the three critical bonds of the Ag−O bonds (about 0.04 e au^{-3}) are smaller by a factor of about two or three than those of the corresponding copper complex **1Cu**$^+$(see Table 2). These values are similar to those reported for other compounds of essentially electrostatic nature, such as formamide-Li^+ or formamide-Na^+,[36] (0.038 and 0.028 e au^{-3}, respectively). This shows that the nature of the O−Ag^+ bonds, is predominantly electrostatic, in contrast to the [glycerol,Cu]$^+$ system, which presents a non-negligible covalent character.

The association of Ag^+ with two oxygen atoms leads to less stable complexes, namely **2Ag**$^+$, **3Ag**$^+$, and **4Ag**$^+$ by 40, 16, and 30 kJ mol^{-1}, respectively. It should be noted that the relative stabilities of these complexes are inverted compared to those of copper ones. Now, the **2Ag**$^+$ structure is less stable than structures **3Ag**$^+$ and **4Ag**$^+$. In the **3Ag**$^+$ complex, Ag^+ is bridging between the O1 and O2 oxygen atoms (2.383 and 2.305 Å). One strong intramolecular hydrogen bond (H2−O3) remains after the complexation of neutral glycerol **A**, as in the case of **3Cu**$^+$. Rotation around C2−C3 bond leads to complex **4Ag**$^+$. The cost for the loss of such a hydrogen bond is about 14 kJ mol^{-1}. In **4Ag**$^+$, the neighboring C−O bonds are lengthened with regard to neutral glycerol **B**, whereas the C1−C2 bond distance decreases. The **2Ag**$^+$ structure corresponds to the symmetrical interaction of Ag^+ with oxygen atoms, O1 and O3 (2.307 Å). In this complex, once more, the lengthening of the terminal C−O bonds regarding the corresponding neutral structure of glycerol (0.020 and 0.027 Å) is observed.

The **5Ag**$^+$ complex corresponds to the association of Ag^+ with the central oxygen atom O2 and lies 97 kJ mol^{-1} above **1Ag**$^+$. The same structural features appear: the central C−O bond of glycerol is elongated (0.047 Å) after complexation, whereas the other C−O bond distances decrease. As in the case of the **5Cu**$^+$ structure, the intramolecular hydrogen bond is reinforced, as shown by the charge density at the corresponding bcp ($\rho = 0.03$ e au^{-3}). The last structure, **6Ag**$^+$, is 65 kJ mol^{-1} higher in energy than **1Ag**$^+$. This structure is very similar to the one found in the case of Cu^+. The only difference with **6Cu**$^+$ is the metal−oxygen distance.

The binding energies for the six [glycerol,Ag]$^+$ complexes are shown in the Table 6. The analysis of the results shows that the behavior of these complexes is similar to that found for [glycerol,Cu]$^+$ complexes. The larger binding energy corresponds to the tricoordinated structure **1Ag**$^+$ (224 kJ mol^{-1}). Then, the binding energies for the dicoordinated complexes are somewhat smaller (209, 196, and 186 kJ mol^{-1} for **3Ag**$^+$, **4Ag**$^+$, and **2Ag**$^+$, respectively). For the sake of comparison, $\Delta G°_{298}$ for the reaction $Ag^+ + 2$ MeOH → $Ag(MeOH)_2^+$ has been evaluated to be about −210 kJ mol^{-1}.[37] Finally, the mono-

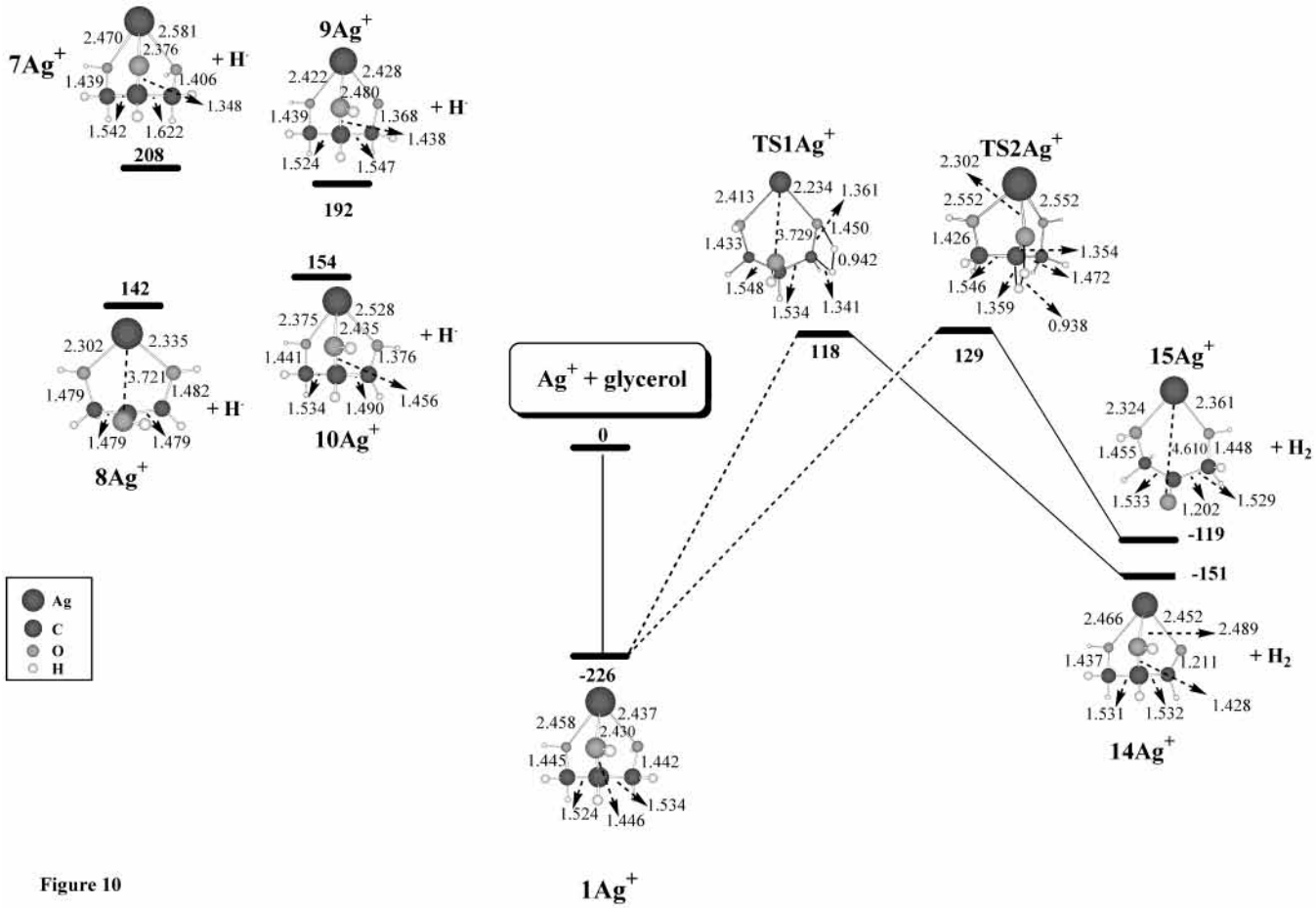

Figure 10

Figure 10. Schematic representation of the potential energy surface associated with several unimolecular reactions of [glycerol,Ag]$^+$ leading to the loss of H· and H_2. Distances are in Angströms and relative energies are in kJ mol^{-1}. B3LYP/basis2 + ZPE energies are shown.

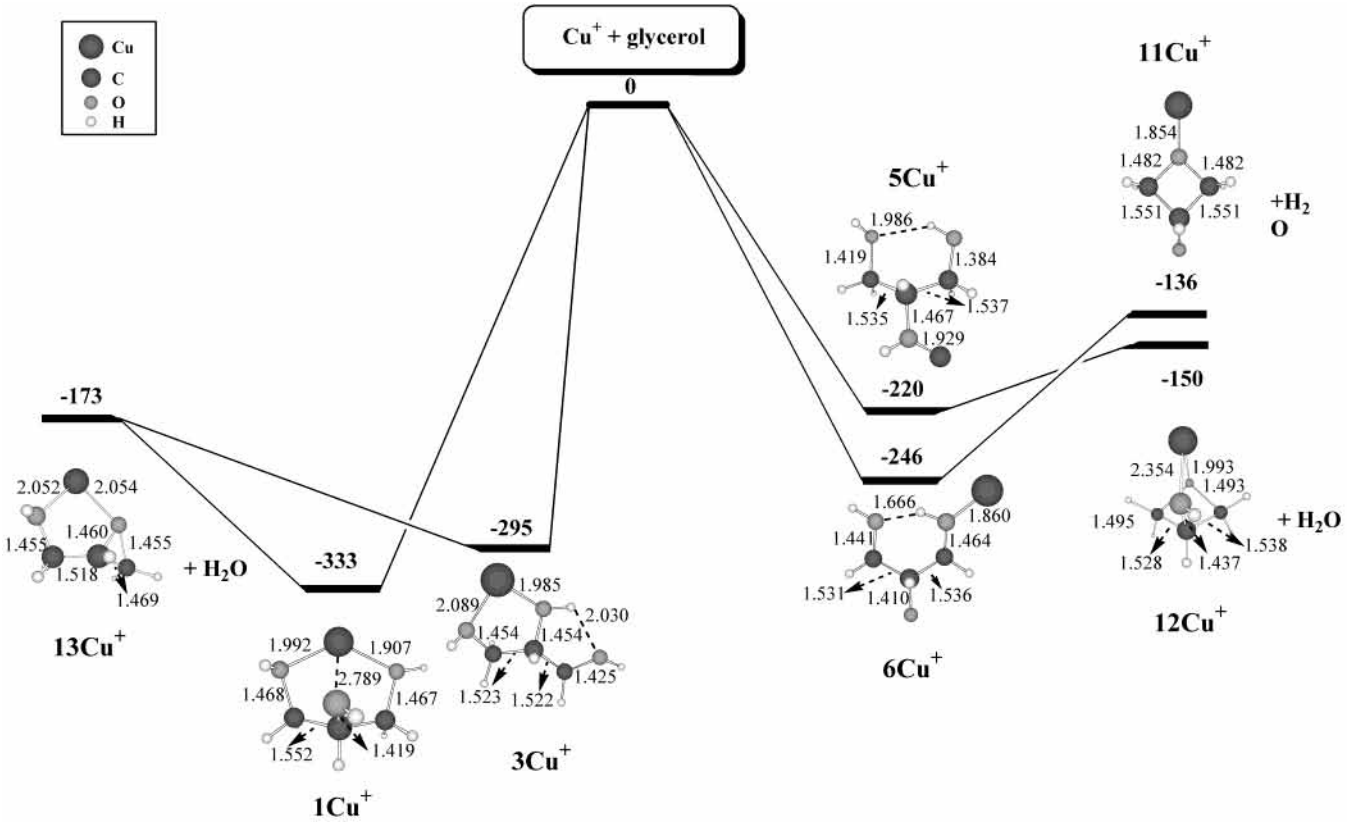

Figure 11. Schematic representation of the potential energy surface associated with several unimolecular reactions of [glycerol,Cu]$^+$ leading to a direct loss of H_2O. Distances are in Angströms and relative energies are in kJ mol^{-1}. B3LYP/basis2 + ZPE energies are shown.

coordinated structures have the smallest values (160 and 132 kJ mol^{-1} for **6Ag**$^+$ and **5Ag**$^+$, respectively). Recently, the binding energy of the silver ion to methanol was calculated (126 kJ mol^{-1}) and measured (138 ± 15.5 kJ mol^{-1}) using the threshold collision-induced dissociation (CID) method.[38] It is worth noting that the affinity of glycerol for Cu^+ is 100 kJ mol^{-1} higher than that for Ag^+.

In summary, interaction with the three basic sites is favored and found to be more stable than complexation on two basic sites. Some differences are observed between Cu^+ and Ag^+ complexation. First, structure **1X**$^+$ (with X = Cu, Ag) is the most stable whatever the implicated cation, but the structure is different depending on the metal cation. In the case of copper cation association, the metal cation is located between O1 and O3, whereas Ag^+ bridges in a similar way with the three oxygen atoms. This difference can be explained in terms of orbital overlapping and electrostatic interactions. Even if these latter cases are predominant, we can assume that the "covalent part" of O−Cu^+ bonding is a combination of the following: (i) a dative bond involving sp hybrids (with a strong p character) of oxygen atoms and appropriate sd hybrids of Cu^+ and (ii) a charge transfer from Cu^+ to oxygen atoms (favored by a quite small ionic radius of Cu^+, R_{Cu^+} = 0.96 Å). According to the bigger ionic radius of Ag^+ (R_{Ag^+} = 1.26 Å) the interaction distance O−Ag^+ is increased by about 0.4 Å, and consequently, the overlap between the lone pairs of oxygen atoms and orbitals 4d of silver are less favorable. Thus, covalent contributions are much less important, or even negligible. Second, for the dicoordinated adducts, **2X**$^+$, **3X**$^+$, and **4X**$^+$, it is important to emphasize that the order of stability is inverted. In other words, Ag^+ prefers to be dicoordinated with vicinal hydroxylic oxygen atoms. As in the case of Cu^+ complexation, the entropy changes have been also evaluated from theory (see Tables 1 and 5). In the case of silver complexes, the values are slightly smaller than the corresponding copper ones and range from −20.8 to −25.9 cal/K mol.

To assess the reliability of the model, we present some preliminary results concerning the most favorable site of complexation of α-D-Glucopyranose by Cu^+ and Ag^+. As annotated in the Introduction, due to the number of conformations and basic centers, the possibilities for complexation of α-D-Glucopyranose are numerous. This has been evidenced in previous works devoted to the complexation of monosaccharides by Na^+,[6h] Li^+, Be^{2+}, Mg^{2+}, and Ca^{2+}.[39] and our works concerning the complexation by Cu^+.[7] Our aim here is to show that glycerol can be a good model for a first approach. In α-D-Glucose, the most favorable site of cationization for both Cu^+ and Ag^+ cations involves, as expected, three oxygen atoms: the hemiacetal, the anomeric hydroxyl, and the hydromethyl. Several dicoordinated structures are possible. We have selected two of them where the complexation modes look like those of glycerol. We can see in Figure 10 that the behavior is similar. In the case of copper structures, the six-membered **α-D-Glu1-Cu**$^+$ structure is more stable by 39 kJ mol^{-1} than the five-membered one **α-D-Glu2-Cu**$^+$, whereas the contrary is observed for corresponding silvered complexes: **α-D-Glu1-Ag**$^+$ being less stable by 13 kJ mol^{-1} than **α-D-Glu2-Ag**$^+$. From these findings, work is in progress to propose the most probable structures that come closest to explain the difference of reactivity induced by the complexation of some monosaccharides by Cu^+ and Ag^+ cations.

Reactivity of the [Glycerol,X]$^+$ Adducts. To rationalize the observed gas-phase reactivity of the [glycerol,X]$^+$ (X = Cu and Ag) complexes, we have envisaged different mechanisms that can account for the most abundant fragmentations obtained in MIKE spectra, namely loss of H•, H_2, H_2O, and glycerol.

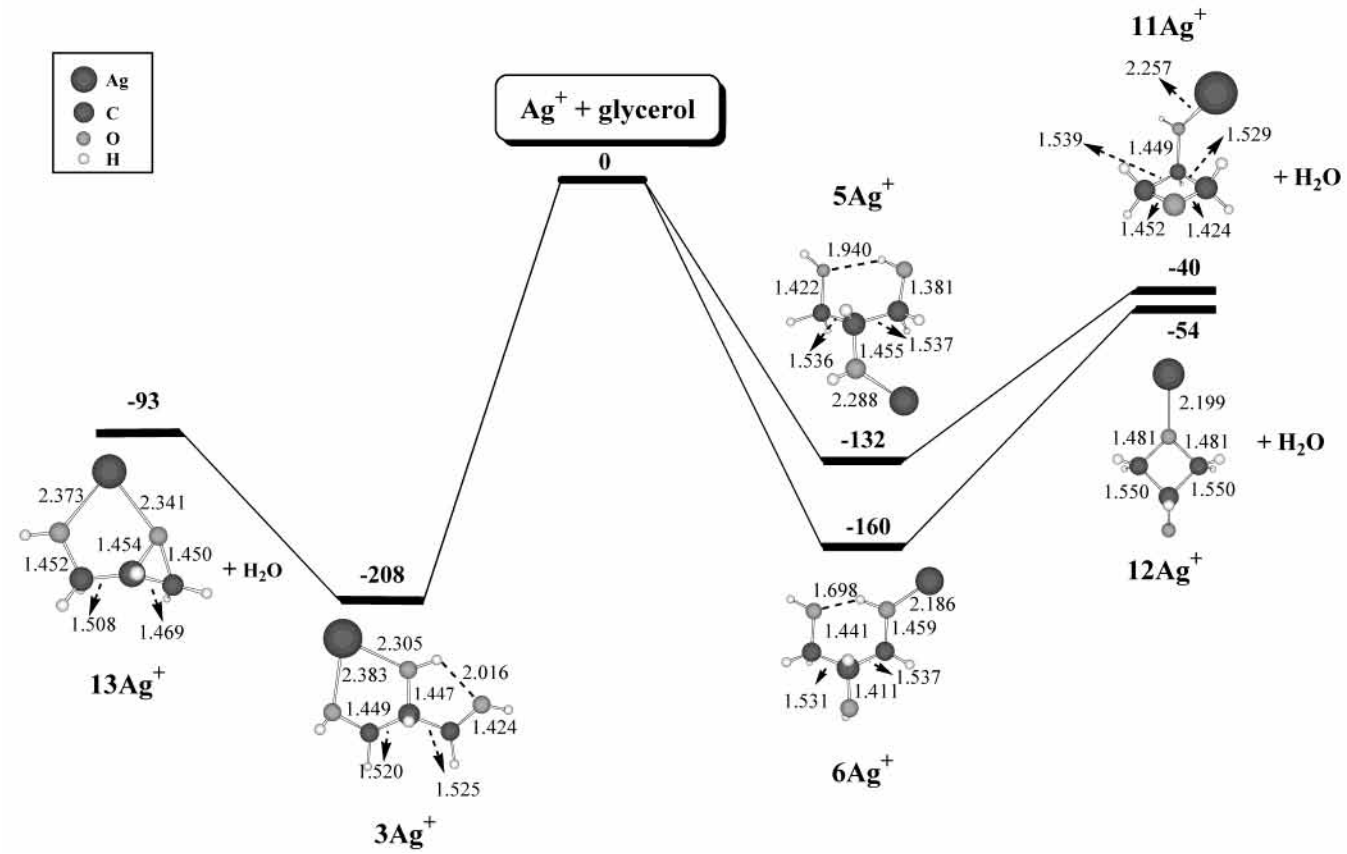

Figure 12. Schematic representation of the potential energy surface associated with several unimolecular reactions of [glycerol,Ag]$^+$ leading to a direct loss of H_2O. Distances are in Angströms and relative energies are in kJ mol^{-1}. B3LYP/basis2 + ZPE energies are shown.

We will first analyze the elimination of H• and H_2. As mentioned previously, the MIKE spectra of deuterated glycerol show that the hydrogen atoms implicated in the elimination of H_2 arise from the hydroxyl and from the CH_2 (CH) groups of glycerol. Figures 9 and 10 display the obtained mechanisms that lead to the elimination of H• and H_2 from the most stable **1Cu**$^+$ and **1Ag**$^+$ structures. Four paths have been investigated for the loss of H• that yield to **7X**$^+$, **8X**$^+$, **9X**$^+$, and **10X**$^+$ + H• (X = Cu and Ag) without barriers in excess. The **7X**$^+$ and **8X**$^+$ structures arise to the elimination of the hydrogen atom from the central OH and from the CH groups, respectively when the **9X**$^+$ and **10X**$^+$ products correspond to the elimination of the H atom from the end OH and from the CH_2 groups, respectively. It can be observed in Figure 9 that several of these pathways leading to the elimination of H• from [glycerol,Cu]$^+$ have energy requirements comparable to the energy of the reactants. Consequently, these mechanisms can be accessible, and a portion of [glycerol,Cu]$^+$ molecules having enough energy can lose H•, as we detect in the MIKE spectrum. In the case of Ag^+, all of the processes leading to the elimination of a hydrogen atom are highly endothermic, as the products are more than 142 kJ mol^{-1} higher in energy than the reactants, as shown in Figure 10. Therefore, this fragmentation is not observed in the spectrum of [glycerol,Ag]$^+$.

Starting from **1X**$^+$, two different pathways for the loss of H_2 are possible. The first one takes place through **TS1X**$^+$, which lies 4 kJ mol^{-1} below the reactants in the case of Cu^+ and 118 kJ mol^{-1} above the reactants in the case of Ag^+. In both cases, this reaction path leads to **14X**$^+$ + H_2 and corresponds to the simultaneous elimination of one hydrogen atom from the CH group and one hydrogen atom from the adjacent hydroxyl. Likewise, the elimination of the hydrogen atoms from the end CH_2 and OH groups leads to **15X**$^+$ + H_2. The transition state connecting both products and reactants is **TS2X**$^+$ and lies 41 kJ mol^{-1} in the case of Cu^+ and 129 kJ mol^{-1} in the case of Ag^+ above the reactants. Thus, for the [glycerol,Cu]$^+$ complex the loss of H_2 can be an accessible pathway as shown by the corresponding peak found in the MIKE spectrum. For the [glycerol,Ag]$^+$, the loss of H_2 is more favorable than the elimination of H•, but the barriers to these pathways are still much higher in energy than those of the reactants. However, a portion of [glycerol,Ag]$^+$ complexes can have an excess of internal energy, which can arise from the collisional activation with the background gas, that would produce the elimination of H_2. It should be pointed out that the loss of H_2 could also come from the fragmentation of other isomers of [glycerol,X]$^+$. In addition, starting from other less stable isomers, we have studied the mechanisms leading to the elimination of H_2, and in all cases the activation barriers are higher in energy than those found for the most stable isomer.

In summary, as shown in Figure 10, the most favorable process for the most stable structure of [glycerol,Ag]$^+$ corresponds to the loss of glycerol in agreement with experimental evidence. Actually, the energy required to dissociate the **1Ag**$^+$ complex is systematically smaller than the activation barriers involved in the remaining alternative mechanisms. For the [glycerol,Cu]$^+$ complex, several mechanisms yielding loss of H• or H_2 are energetically accessible. Also, one can emphasize that the dissociation of [glycerol,Cu]$^+$ into Cu^+ + glycerol is not observed in the MIKE spectrum. Therefore, a small excess of internal energy into our systems, would favor the elimination of H• and H_2 in the case of [glycerol,Cu]$^+$ and the dissociation of [glycerol,Ag]$^+$ into Ag^+ + glycerol.

Concerning the loss of water, as mentioned abvove, the MIKE spectra of complexes obtained by using deuterated glycerol show that the hydrogen atoms involved in this fragmentation come

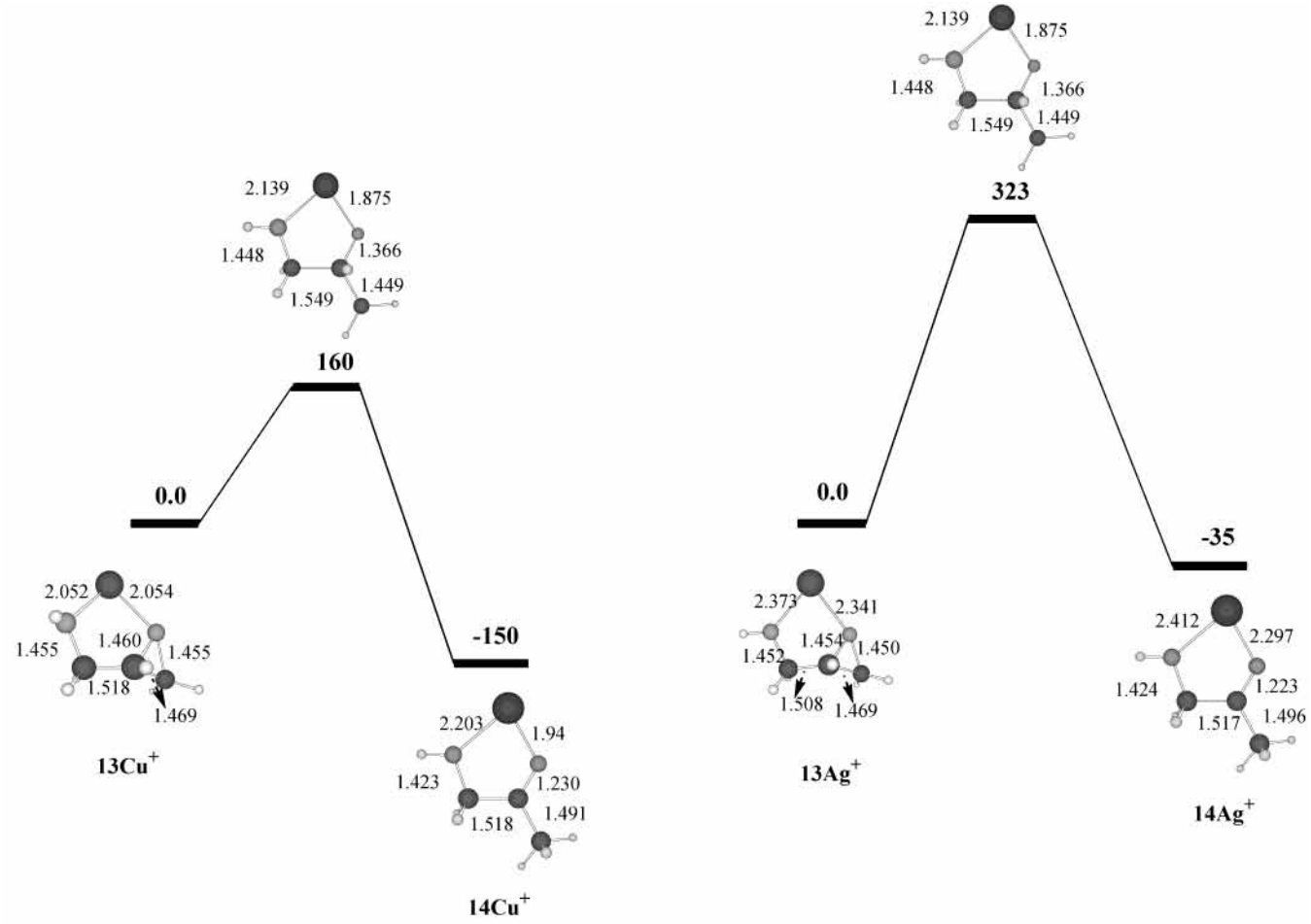

Figure 13. Schematic representation of the potential energy surface associated with $\mathbf{13X}^+ \rightarrow \mathbf{14X}^+$ isomerization. Relative energies are in kJ mol^{-1}. B3LYP/basis2 + ZPE energies are shown.

from two of the three hydroxyl groups of glycerol. Thus, to obtain the elimination of water, a hydrogen atom has to be transferred from one hydroxyl group to another one. Because of the presence of a hydrogen bond, structures $\mathbf{3X}^+$, $\mathbf{5X}^+$, and $\mathbf{6X}^+$ (see Figures 6 and 7) are the ones in which the hydrogen transfer is possible. Moreover, as noted before, in all of the structures, the acidic character of the hydrogen donor oxygen increases after complexation, thus favoring the proton transfer. So, part of the observed reactivity of the $[glycerol,X]^+$ complexes can arise from structures different from the most stable one. Figures 11 and 12 show a possible mechanism that can lead to the elimination of H_2O. Similar trends are found for both $[glycerol,Cu]^+$ and $[glycerol,Ag]^+$ systems. In all cases, the loss of H_2O is a favorable process regarding the reactants X^+ + glycerol. Starting from isomer $\mathbf{3X}^+$, a direct transfer of a hydrogen atom from O2 to O3 leads to $\mathbf{13X}^+ + H_2O$ without activation barrier. All attempts to locate a complex with the hydrogen atom transferred to the O3 oxygen failed because, in all cases, the H_2O molecule dissociates directly, yielding $\mathbf{13X}^+ + H_2O$. In the same way, departing from $\mathbf{5X}^+$ and $\mathbf{6X}^+$, a hydrogen transfer from O3 to O1 leads also to a direct elimination of H_2O. Because of the strain of the three-member ring, we have envisaged the isomerization of $\mathbf{13X}^+$. Departing from $\mathbf{13X}^+$ the ring opening followed by a hydrogen atom transfer gives rise, through the appropriate transition state, to the hydroxyacetone-X^+ complexes $\mathbf{14Cu}^+$ and $\mathbf{14XAg}^+$ (see Figure 13). Both structures are more stable by 150 and 35 kJ mol^{-1} than $\mathbf{13Cu}^+$and $\mathbf{13Ag}^+$ respectively. Nevertheless, it is worth noting that the barriers are significant, especially for the Ag^+ complex. Actually, the corresponding transition states lie 150 kJ and 323 kJ above $\mathbf{13Cu}^+$ and $\mathbf{13Ag}^+$ respectively. For Ag^+ complexes, one can put forward that the isomerization process does not take place.

Starting from $\mathbf{1X}^+$, a second possibility has been considered for water loss. We have explored a stepwise mechanism, already suggested by Allison and Ridge,[40] that involves, as intermediate, a three coordinate species i.e., a [hydroxyacetone-X^+-H_2O] complex (see Figure 14). Thus, departing from the more stable complex $\mathbf{1X}^+$, the first step corresponds to a direct transfer of a hydroxyl group from CH_2-OH to the metal ion, leading to a complex noted as $\mathbf{15X}^+$. This structure corresponds to a tetracoordinated species, which lies 51 kJ mol^{-1} above $\mathbf{1Cu}^+$ and 292 kJ mol^{-1} above $\mathbf{1Ag}^+$. It is worth nothing that $\mathbf{15Ag}^+$- is 66 kJ mol^{-1} above the reactants Ag^+ + glycerol. Thus, this reaction path is thermodynamically unfavorable for Ag^+ complexation, and in agreement with experimental findings water elimination cannot take place from such a reaction.

In the case of Cu^+, as shown in Figure 14, the transition state connecting both minima $\mathbf{1Cu}^+$ and $\mathbf{15Cu}^+$ is 246 kJ mol^{-1} below the reactants Cu^+ + glycerol. From $\mathbf{15Cu}^+$, a 1,2-hydrogen transfer, from CH(OH) group to CH_2 group, gives rise (through a barrier of 152 kJ mol^{-1}) to $\mathbf{16Cu}^+$, in which the Cu atom forms a four member ring. This structure is more stable than $\mathbf{15Cu}^+$ by 23 kJ mol^{-1}. Through an energy barrier of 68 kJ mol^{-1}, the transfer of the hydroxyl hydrogen atom C2(O**H**) to the metal ion leads directly to the global minimum of the PES, namely $\mathbf{17Cu}^+$. In this structure, Cu^+ is coordinated both to a molecule of water and to a molecule of hydroxyacetone. It

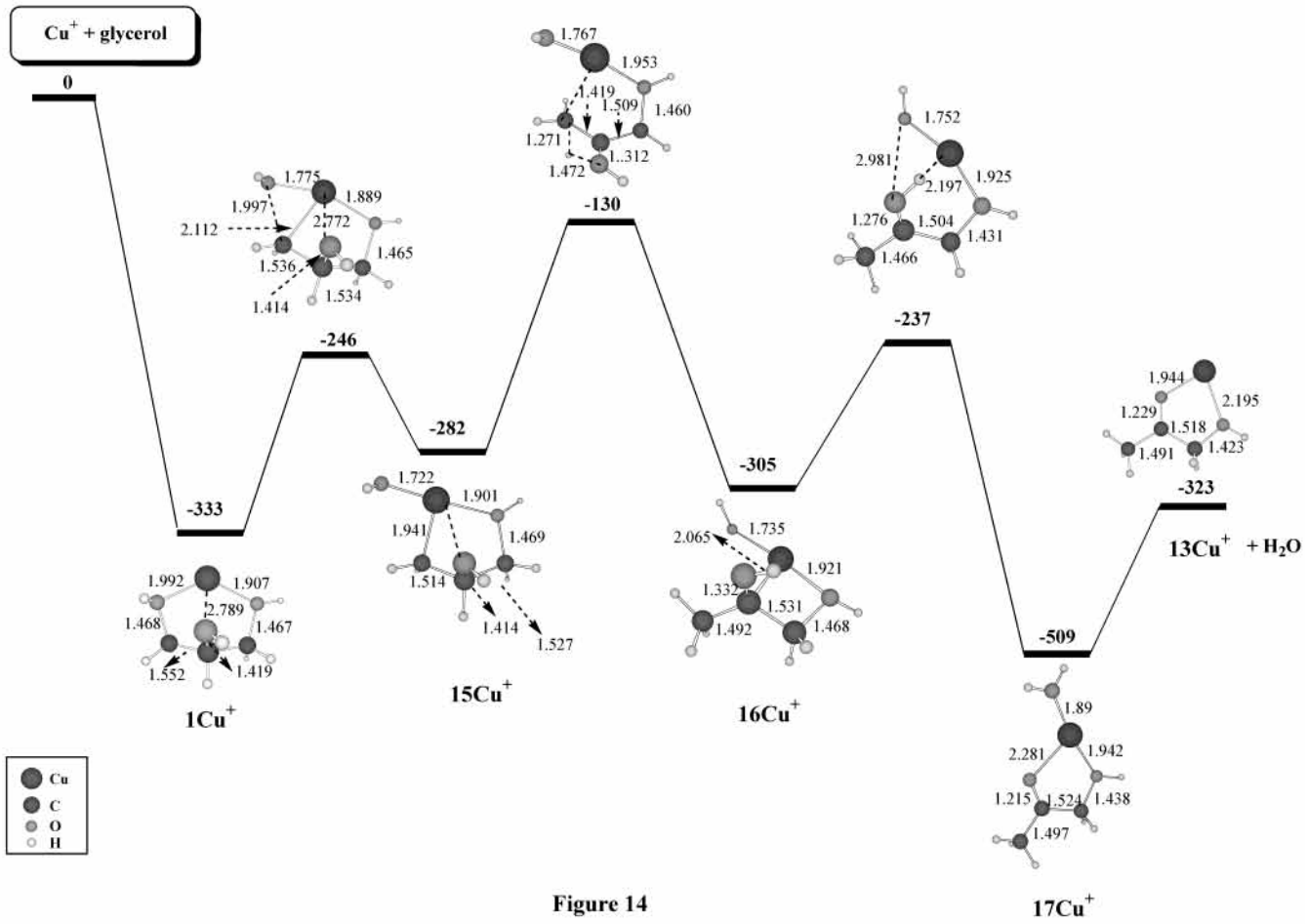

Figure 14. Schematic representation of the potential energy surface associated with the loss of water from [glycerol,Cu]$^+$. Distances are in Angströms and relative energies are in kJ mol^{-1}. B3LYP/basis2 + ZPE energies are shown.

can evolve without energy barrier to the elimination of H_2O. As a summary, one can point out, as shown in Figure 14, that all of the intermediates involved in this mechanism are thermodynamically accessible. Thus, without kinetic considerations, this stepwise mechanism can compete with the direct elimination of water displayed in Figure 12.

4. Concluding Remarks

Reactions between glycerol and X^+ (X = Cu and Ag) in the gas phase under FAB conditions produce the [glycerol,Cu]$^+$ and [glycerol,Ag]$^+$ adducts. The different isomers of these adducts have been investigated by means of the B3LYP theoretical approach. Several coordinations of the metal cation to the basic sites of glycerol have been considered. The most stable structure corresponds to the interaction of Cu^+ with two oxygen atoms of glycerol and to the Ag^+ ion interacting with the three oxygen atoms of glycerol. The estimated Cu^+-glycerol D_e binding energy (333 kJ mol^{-1}) is similar to the values obtained for other Cu^+ complexes, such as Cu^+-glycine or Cu^+-guanidine calculated at similar levels. The binding energy for Ag^+-glycerol is about 100 kJ mol^{-1} smaller than that of Cu^+-glycerol.

The unimolecular reactivity of the [glycerol,X]$^+$ (X = Cu and Ag) ions has also been studied both experimentally and theoretically. The MIKE spectra show differences between Cu^+ and Ag^+ complexes. The major fragmentation of the [glycerol,Cu]$^+$ ion corresponds to the elimination of H_2O. Other losses are also observed namely that of H· and H_2. However, the major fragmentation of [glycerol,Ag]$^+$ corresponds to the loss of the ligand process. The elimination of H_2 and H_2O are also observed, as in the case of [glycerol,Cu]$^+$. The MIKE spectra of deuterated glycerol show that in both cases the hydrogen atoms implicated in the loss of H_2O come from two hydroxyl groups. Nevertheless, the loss of H_2 involves one hydroxyl oxygen atom and one atom arising from CH_2 (or CH) group. Theoretical calculations show that in the case of [glycerol,Cu]$^+$ several pathways leading to the loss of H· or H_2 are potentially accessible. Thus, a small excess of internal energy into the system would lead to the elimination of H· and H_2 and not to the loss of glycerol. This fact accounts for the absence of the peak corresponding to Cu^+ in the MIKE spectrum of [glycerol,Cu]$^+$.

However, all the pathways leading to the loss of H· from the most stable **1Ag**$^+$ structure of [glycerol,Ag]$^+$ are highly endothermic, and the mechanisms leading to the elimination of H_2 exhibit high energy barriers. Therefore, the most favorable reaction for the most stable **1Ag**$^+$ isomer of [glycerol,Ag]$^+$ is the loss of the ligand process.

The peak corresponding to the loss of a water molecule presents very different intensities in the spectra of both cations, being much more intense in the case of Cu^+. Two distinct pathways have been envisaged. The first one involves a hydrogen transfer followed by the direct elimination of water. In the case of [glycerol,Cu]$^+$ the most stable **1Cu**$^+$ structure can undergo fragmentation, when in the case of [glycerol,Ag]$^+$ only fragmentations originated from other less stable isomers of [glycerol,Ag]$^+$, namely **3Ag**$^+$, **5Ag**$^+$, and **6Ag**$^+$, can account for the elimination of water. The second mechanism involves the transfer of a hydroxyl group to the metal ion that yields to

the key intermediate $\mathbf{15X}^+$. The difference of stability of both structures $\mathbf{15Ag}^+$ and $\mathbf{15Cu}^+$ with regard to reactants (glycerol + $Ag^+/Cu^{+)}$ could explain the difference of reactivity. Thus, H_2O loss prevails to the copper complex, whereas glycerol loss is much easier than dehydration for silver.

Acknowledgment. This work has been partially supported by an allocation of computational time from the Institut de Développement et de Recherche (IDRIS Orsay France) and by a NATO cooperative grant (CRG 973140). L. R. acknowledges a postdoctoral Marie Curie grant from the EU.

References and Notes

(1) (a) *Organometallic Ion Chemistry*; Freiser, B. S., Ed.; Kluwer Academic Publishers: Dordrecht, 1996. (b) Armentrout, P. B.; Baer, T. *J. Phys. Chem. A*, **1996**, *100*, 12 866, and references therein. (c) Eller, K.; Schwarz, H. *Chem. Rev.* **1991**, *91*, 1121. (d) Eller, K. *Coord. Chem. Rev.* **1993**, *126*, 93.

(2) (a) Luna, A.; Amekraz, B.; Tortajada, J.; Morizur, J.-P.; Alcamí, M.; Mó, O.; Yáñez, M. *J. Am. Chem. Soc.* **1998**, *120*, 5411. (b) Alcamí, M.; Mó, O.; Yáñez, M.; Luna, A.; Morizur, J.-P.; Tortajada, J. *J. Phys. Chem. A* **1998**, *102*, 10 120.

(3) Luna, A.; Amekraz, B.; Morizur, J.-P.; Tortajada, J.; Mó, O.; Yáñez, M. *J. Phys. Chem. A* **1997**, *101*, 5931.

(4) Luna, A.; Amekraz, B.; Morizur, J.-P.; Tortajada, J.; Mó, O.; Yáñez, M. *J. Phys. Chem. A* **2000**, *104*, 3132.

(5) (a) Luna, A.; Gevrey, S.; Tortajada, J. *J. Phys. Chem. B* **2000**, *104*, 110.

(6) (a) Zhou, Z.; Ogden, S.; Leary, J. A. *J. Org. Chem.* **1990**, *55*, 5444. (b). Dongré, A. R.; Wysocki, V. H. *Org. Mass Spectrom.* **1994**, *29*, 700. (c) Sible, E. M.; Brimmer, S. P.; Leary, J. A. *J. Am. Soc. Mass Spectrom.* **1997**, *8*, 32. (d) Asam, M. R.; Glish, G. L. *J. Am. Soc. Mass Spectrom.* **1997**, *8*, 987. (e) König, S.; Leary, J. A. *J. Am. Soc. Mass Spectrom.* **1998**, *9*, 1125. (f) Berjeaud, J. M.; Couderc, F.; Promé, J−C. *Org. Mass Spectrom.* **1993**, *28*, 455. (g) Madhusudanan, K. P.; Dhami, T. S.; Katiyar, S.; Suryawanshi, S. N. *Org. Mass Spectrom.* **1994**, *29*, 238. (h). Cerda, B. A.; Wesdemiotis, C. *Int. J. Mass Spectrom.* **1999**, *189*, 189. (i) Gaucher, S. P.; Leary, J. A. *Anal. Chem.* **1998**, *70*, 3009. (j) Desaire, H.; Leary, J. A. *Anal. Chem.* **1999**, *71*, 1997. (k) Smith, G.; Kaffashan, A.; Leary, J. A. *Int. J. Mass Spectrom.* **1999**, *182/183*, 299. (l) Carlasso, V.; Fournier, F.; Tabet, J.-C. *Eur. J. Mass Spectrom.* **2000**, *6*, 421.

(7) (a) Salpin, J.-Y.; Boutreau, L.; Haldys, V.; Tortajada, *J. Eur. Mass Spectrom.* **2001**, *7*, 321. (b) Boutreau, L.; Tortajada, J., Luna, A.; Alcami, M.; Mó, O.; Yáñez, M. *Int. J. Quantum Chem.* **2002**, *86*, 138. (c) Alcami, M.; Luna, A.; Mó, O.; Yáñez, M.; Boutreau, L.; Tortajada, J. *J. Phys. Chem. A* **2002**, *106*, 2641.

(8) (a) Ligon, W. V.; Dorn, S. B. *Int. J. Mass Spectrom. Ion Processes* **1986**, *78*, 99. (b) De Pauw, E. *Mass Spectrom. Rev.* **1986**, *5*, 191.

(9) (a) Karlin, K. D.; Tyeklar, Z. Eds.; *Bioinorganic Chemistry of Copper*; Chapman & Hall: New York, 1993. (b) Karlin, K. D.; Zubieta, J. *Biological and Inorganic Copper Chemistry*; Adenine: Guilderland, New York, 1986; Vols I and II. (c) Karlin, K. D.; Zubieta, J. *Copper Coordination Chemistry: Biological and Inorganic Perspectives*; Adenine: Guilderland, New York, 1983.

(10) (b) Wigley, R. A.; Brooks, R. R. *Noble Metals and Biological Systems*; Brooks, R. R., Ed; CRC: Boca Raton, 1992, p 277.

(11) (a) Nomiya, K.; Kondoh, Y.; Nagano, H.; Oda, M. *J. Chem. Soc. Chem. Commun.* **1995**, 1679−1680. (b) Nomiya, K.; Onoue, K. I.; Kondoh, Y.; Kasuga, N. C.; Nagano, H.; Oda, M.; Sakuma, S. *Polyhedron* **1995**, *14*, 1359−1367.

(12) (a) Chu, I. K.; Shoeib, T.; Guo, X.; Rodriquez, C. F.; Hopkinson, A. C.; Siu, K. W. M.; Lau, T. C. *J. Am. Soc. Mass Spectrom.* **2001**, *12*, 163. (b) Shoeib, T.; Cunje, A.; Hopkinson, A. C.; Siu, K. W. M. *J. Am. Soc. Mass Spectrom.* **2002**, *13*, 408. (c) El-Nahas, A. M.; Tajina, N.; Hirao, K. *J. Mol. Struct. (THEOCHEM)* **1999**, *469*, 201. (d) Shoeib, T.; Rodriquez, C. F.; Siu, K. W. M.; Hopkinson, A. C. *J. Chem.* **2001**, *3*, 853. (e) Perera, B. A.; Gallardo, A. L.; Barr, J. M.; Tekarli, S. M.; Anbalagan, V.; Talaty, E. R.; Van Stipdonk, M. J. *J Mass Spectrom.* **2002**, *37*, 401.

(13) Luna, A.; Amekraz, B.; Tortajada, J. *Chem. Phys. Lett.* **1997**, *266*, 31.

(14) Babinec, S. J.; Allison, J. J. *J. Am. Chem. Soc.* **1984**, *106*, 7718.

(15) (a) Burnier, R. C.; Byrd, Freiser, B. S. *Anal. Chem.* **1980**, *52*, 1641 (b) Holland, P. M.; Castelman, A. W. *J. Chem. Phys.* **1982**, *76*, 4195.

(16) Harrison, A. G.; Mercer, R. S.; Reinee, E. J.; Young, A. B.; Boyd, R. K.; March, R. E.; Porter, C. J. *Int. J. Mass Spectrom. Ion Process*. **1986**, *74*, 13.

(17) Dean, I. K. L.; Bush, K. L. *Org. Mass Spectrom*. **1988**, *24*, 733.

(18) (a) Cooks, R. G.; Beynon, J. H.; Caprioli, R. M.; Lester, G. R. *Metastable Ions*; Elsevier: New York, 1973. (b) Cooks, R. G., Ed. *Collision Spectroscopy*; Plenum Press: New York; 1978.

(19) (a) Becke, A. D. *J. Chem. Phys*. **1993**, *98*, 5648. (b) Lee, C.; Yang, W.; Parr, R. G. *Phys. Rev. B* **1988**, *37*, 785. (c) Stevens, P. J.; Devlin, F. J.; Chablowski, C. F.; Frisch, M. J. *J. Phys. Chem.* **1994**, *98*, 11 623.

(20) Holthausen, M. C.; Heineman, C.; Cornehl, H. H.; Koch, W.; Schwarz, H. *J. Chem. Phys*. **1995**, *102*, 4931.

(21) Adamo, C.; Lelj. F. *J. Chem. Phys*. **1995**, *103*, 10 605.

(22) Blomberg, M. R. A.; Siegbahn, P. E. M.; Svensson, M. *J. Chem. Phys*. **1996**, *104*, 9546.

(23) Rodríguez-Santiago, L.; Sodupe, M.; Branchadell, V. *J. Chem. Phys.* **1996**, *105*, 9966.

(24) Bauschlicher, C. W.; Ricca, A.; Partridge, H.; Langhoff, S. R. in *Recent Advances in Density Functional Theory*, Part II.; D. P. Chong, Ed.; World Scientific Publishing Company: Singapore 1997.

(25) (a) Watchers, A. J. H. *J. Chem. Phys.* **1970**, *52*, 1033. (b) Hay, P. J. *J. Chem. Phys.* **1977**, *66*, 4377.

(26) Hay, P. J.; Wadt, R. W. *J. Chem. Phys.* **1985**, *82*, 299.

(27) (a) Hertwig, R. H.; Koch, W.; Schröder, D.; Schwarz, H.; Hrusák, J.; Schwerdtfeger, P. *J. Phys. Chem.* **1996**, *100*, 12 253. (b) Amekraz, B.; Tortajada; J.; Morizur, J.-P.; González, A. I.; Mó, O.; Yáñez, M., *J. Mol. Struct. (THEOCHEM)* **1996**, *371*, 313.

(28) Bader, R. F. W. *Atoms in Molecules. A Quantum Theory*, Oxford University Press: Oxford, U.K. 1990.

(29) Frisch, M. J.; Trucks, G. W.; Schlegel, H. B.; Scuseria, G. E.; Robb, M. A.; Cheeseman, J. R.; Zakrzewski, V. G.; Montgomery, J. A., Jr.; Stratmann, R. E.; Burant, J. C.; Dapprich, S.; Millam, J. M.; Daniels, A. D.; Kudin, K. N.; Strain, M. C.; Farkas, O.; Tomasi, J.; Barone, V.; Cossi, M.; Cammi, R.; Mennucci, B.; Pomelli, C.; Adamo, C.; Clifford, S.; Ochterski, J.; Petersson, G. A.; Ayala, P. Y.; Cui, Q.; Morokuma, K.; Malick, D. K.; Rabuck, A. D.; Raghavachari, K.; Foresman, J. B.; Cioslowski, J.; Ortiz, J. V.; Stefanov, B. B.; Liu, G.; Liashenko, A.; Piskorz, P.; Komaromi, I.; Gomperts, R.; Martin, R. L.; Fox, D. J.; Keith, T.; Al-Laham, M. A.; Peng, C. Y.; Nanayakkara, A.; Gonzalez, C.; Challacombe, M.; Gill, P. M. W.; Johnson, B. G.; Chen, W.; Wong, M. W.; Andres, J. L.; Head-Gordon, M.; Replogle, E. S.; Pople, J. A. *Gaussian 98*, revision A.7; Gaussian, Inc.: Pittsburgh, PA, 1998.

(30) The AIMPAC Programs package was provided by J. Cheeseman and R. F. W. Bader.

(31) Chelli, R.; Gervasio, F. L.; Gellini, C.; Procacci, P.; Cardini, G.; Schettino, V. *J. Phys. Chem. A* **2000**, *104*, 11 220.

(32) Callam, C. S.; Sherwin, J. S.; Lowary, T. L.; Hadad, C. M. *J. Am. Chem. Soc.* **2001**, *123*, 11 754.

(33) Hoyau, S.; Ohanessian, G. *J. Am. Chem. Soc*. **1997**, *119*, 2016.

(34) Deng, H.; Kebarle, P. *J. Am. Chem. Soc*. **1998**, *120*, 2925.

(35) Hoyau, S.; Ohanessian, G. *Chem. Phys. Lett.* **1997**, *280*, 266.

(36) Tortajada, J.; Léon E.; Morizur, J.-P.; Luna, A.; Mó, O.; Yáñez, M. *J. Phys. Chem*. **1995**, *99*, 13 890.

(37) Deng, H.; Kebarle, P. *J. Phys. Chem.* **1998**, *102*, 571.

(38) El Aribi, H.; Shoeib, T.; Ling, Y.; Rodriquez, C. F.; Hopkinson, A. C.; Siu, K. W. M. *J. Phys. Chem. A* **2002**, *106*, 2908.

(39) Zheng, Y.-J.; Ornstein, R. L.; Leary, J. A. *J. Mol. Struct (THEOCHEM)* **1997**, *389*, 233.

(40) Allison, J.; Ridge, D. P. *J. Am. Chem. Soc*. **1979**, *101*, 4998.